EUROPEAN ORGANIZATION FOR NUCLEAR RESEARCH (CERN)

CERN-EP/2016-036
2016/05/13

CMS-SUS-15-002

Search for supersymmetry in the multijet and missing transverse momentum final state in pp collisions at 13 TeV

The CMS Collaboration*

arXiv:1602.06581v2 [hep-ex] 11 May 2016

Abstract

A search for new physics is performed based on all-hadronic events with large missing transverse momentum produced in proton-proton collisions at $\sqrt{s} = 13$ TeV. The data sample, corresponding to an integrated luminosity of 2.3 fb^{-1}, was collected with the CMS detector at the CERN LHC in 2015. The data are examined in search regions of jet multiplicity, tagged bottom quark jet multiplicity, missing transverse momentum, and the scalar sum of jet transverse momenta. The observed numbers of events in all search regions are found to be consistent with the expectations from standard model processes. Exclusion limits are presented for simplified supersymmetric models of gluino pair production. Depending on the assumed gluino decay mechanism, and for a massless, weakly interacting, lightest neutralino, lower limits on the gluino mass from 1440 to 1600 GeV are obtained, significantly extending previous limits.

Published in Physics Letters B as doi:10.1016/j.physletb.2016.05.002.

© 2016 CERN for the benefit of the CMS Collaboration. CC-BY-3.0 license

*See Appendix C for the list of collaboration members

1 Introduction

The standard model (SM) of particle physics successfully describes a wide range of phenomena. However, in the SM, the Higgs boson mass is unstable to higher-order corrections, suggesting that the SM is incomplete. Many extensions to the SM have been proposed to provide a more fundamental theory. Supersymmetry (SUSY) [1–8], one such extension, postulates that each SM particle is paired with a SUSY partner from which it differs in spin by one-half unit. As examples, squarks and gluinos are the SUSY partners of quarks and gluons, respectively, while neutralinos $\widetilde{\chi}^0$ (charginos $\widetilde{\chi}^{\pm}$) arise from a mixture of the SUSY partners of neutral (charged) Higgs and electroweak gauge bosons. Radiative corrections involving SUSY particles can compensate the contributions from SM particles and thereby stabilize the Higgs boson mass. For this cancellation to be "natural" [9–12], the top squark, bottom squark, and gluino must have masses on the order of a few TeV or less, possibly allowing them to be produced at the CERN LHC.

Amongst SUSY processes, gluino pair production, typically yielding four or more hadronic jets in the final state, has the largest potential cross section, making it an apt channel for early SUSY searches in the recently started LHC Run 2. Furthermore, in R-parity [13] conserving SUSY models, as are considered here, the lightest SUSY particle (LSP) is stable and assumed to be weakly interacting, leading to potentially large undetected, or "missing", transverse momentum. Supersymmetry events at the LHC might thus be characterized by significant missing transverse momentum, numerous jets, and — in the context of natural SUSY — jets initiated by top and bottom quarks.

This Letter describes a search for gluino pair production in the all-hadronic final state. The data, corresponding to an integrated luminosity of 2.3 fb^{-1} of proton-proton collisions at a center-of-mass energy of $\sqrt{s} = 13\,\text{TeV}$, were collected with the CMS detector in 2015, the initial year of the LHC Run 2. Recent searches for gluino pair production at $\sqrt{s} = 8\,\text{TeV}$, based on data collected in LHC Run 1, are presented in Refs. [14–16]. Because of the large mass scales and their all-hadronic nature, the targeted SUSY events are expected to exhibit large values of H_T, where H_T is the scalar sum of the transverse momenta (p_T) of the jets. As a measure of missing transverse momentum, we use the variable H_T^miss, which is the magnitude of the vector sum of the jet p_T. We present a general search for gluino pair production leading to final states with large H_T, large H_T^miss, and large jet multiplicity. The data are examined in bins of N_jet, $N_\text{b-jet}$, H_T, and H_T^miss, where N_jet is the number of jets and $N_\text{b-jet}$ the number of tagged bottom quark jets (b jets). The search is performed in exclusive bins of these four observables.

We consider SUSY scenarios in the context of four simplified models [17–20] of new particle production. Diagrams for the four models are shown in Fig. 1. Simplified models contain the minimal particle content to represent a topological configuration. As SUSY production scenarios, the four simplified models can be interpreted as follows. In the first scenario, shown in Fig. 1 (upper left), gluino pair production is followed by the decay of each gluino to a bottom quark and an off-shell bottom squark. The off-shell bottom squark decays to a bottom quark and the LSP, where the LSP is assumed to be the lightest neutralino $\widetilde{\chi}_1^0$ and to escape detection, leading to significant H_T^miss. The second scenario, shown in Fig. 1 (upper right), is the same as the first scenario except with top quarks and off-shell top squarks in place of the bottom quarks and squarks. The third scenario, shown in Fig. 1 (lower left), is the corresponding situation with gluino decay to a light-flavored quark and off-shell-squark: up, down, strange, and charm with equal probability, for each gluino separately. In the fourth scenario, shown in Fig. 1 (lower right), also based on gluino pair production, each gluino similarly decays to a light-flavored quark and corresponding off-shell squark. The off-shell squark decays to a quark

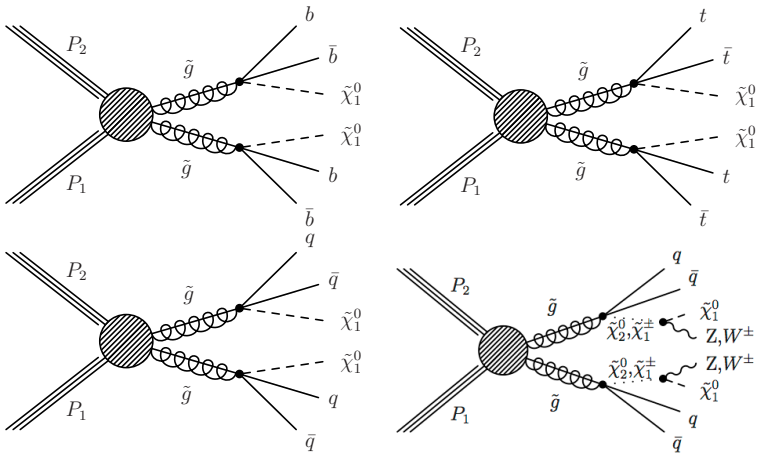

Figure 1: Event diagrams for the new-physics scenarios considered in this study: the (upper left) T1bbbb, (upper right) T1tttt, (lower left) T1qqqq, and (lower right) T5qqqqVV simplified models. For the T5qqqqVV model, the quark q and antiquark $\bar{q}$ do not have the same flavor if the gluino $\tilde{g}$ decays as $\tilde{g} \to q\bar{q}\tilde{\chi}_1^\pm$, with $\tilde{\chi}_1^\pm$ a chargino.

and to either the next-to-lightest neutralino $\tilde{\chi}_2^0$ or the lightest chargino $\tilde{\chi}_1^\pm$. The probability for the decay to proceed via the $\tilde{\chi}_2^0$, $\tilde{\chi}_1^+$, or $\tilde{\chi}_1^-$, integrated over the event sample, is 1/3 for each possibility. The $\tilde{\chi}_2^0$ ($\tilde{\chi}_1^\pm$) subsequently decays to the $\tilde{\chi}_1^0$ LSP and to a on- or off-shell Z ($W^\pm$) boson. We refer to the four simplified models as the T1bbbb, T1tttt, T1qqqq, and T5qqqqVV scenarios, respectively [21]. Thus the first two scenarios explicitly presume either bottom or top squark production. The latter two scenarios represent more inclusive situations and provide complementary sensitivity to top squark production for large values of N_{jet}. We assume all SUSY particles other than the gluino, the LSP, and — for the T5qqqqVV models — the $\tilde{\chi}_2^0$ and $\tilde{\chi}_1^\pm$, to be too heavy to be directly produced, and the gluino to be short-lived.

The principal sources of background arise from the SM production of top quarks, a W or Z boson in association with jets (W+jets or Z+jets events), and multiple jets through the strong interaction. We refer to the latter class of background as quantum chromodynamics (QCD) multijet events. The events with top quarks mostly arise from top quark-antiquark ($t\bar{t}$) production, but also from single top quark processes. The W and Z bosons in W+jets and Z+jets events can be either on- or off-shell. For top quark and W+jets events, significant $H_{\text{T}}^{\text{miss}}$ can arise if a W boson decays leptonically, producing a neutrino and an undetected charged lepton, while Z+jets events can exhibit significant $H_{\text{T}}^{\text{miss}}$ if the Z boson decays to two neutrinos. For QCD multijet events, significant $H_{\text{T}}^{\text{miss}}$ can arise if the event contains a charm or bottom quark that undergoes a semileptonic decay, but the principal source of $H_{\text{T}}^{\text{miss}}$ is the mismeasurement of jet p_{T}.

This study combines and extends search strategies developed for the analysis of CMS data collected at $\sqrt{s} = 8$ TeV, specifically the study of Ref. [22], which examined data in bins of $N_{\text{b-jet}}$ but not N_{jet} and proved to be sensitive to the T1bbbb scenario, and the study of Ref. [23], which examined data in bins of N_{jet} but not $N_{\text{b-jet}}$ and proved to be sensitive to the T1tttt, T1qqqq, and T5qqqqVV scenarios. Here, the two approaches are combined in a unified framework to yield a more comprehensive and inclusive study with improved sensitivity.

2 Detector, trigger, and event reconstruction

The CMS detector is built around a superconducting solenoid of 6 m internal diameter, providing a magnetic field of 3.8 T. Within the solenoid volume are a silicon pixel and strip tracker, a lead tungstate crystal electromagnetic calorimeter (ECAL), and a brass and scintillator hadron calorimeter (HCAL). The ECAL and HCAL, each composed of a barrel and two endcap sections, extend over a pseudorapidity range $|\eta| < 3.0$. Forward calorimeters on each side of the interaction point encompass $3.0 < |\eta| < 5.0$. The tracking detectors cover $|\eta| < 2.5$. Muons are measured within $|\eta| < 2.4$ by gas-ionization detectors embedded in the steel flux-return yoke outside the solenoid. The detector is nearly hermetic, permitting accurate measurements of $H_{\mathrm{T}}^{\mathrm{miss}}$. A more detailed description of the CMS detector, together with a definition of the coordinate system and relevant kinematic variables, is given in Ref. [24].

Signal event candidates are recorded using trigger conditions based on thresholds on H_{T} and missing transverse momentum. The trigger efficiency, which exceeds 98% following application of the event selection criteria described below, is measured in data and is accounted for in the analysis. Separate data samples requiring the presence of either charged leptons or photons are used for the determination of backgrounds from SM processes, as discussed below.

Physics objects are defined using the particle-flow (PF) algorithm [25, 26], which reconstructs and identifies individual particles through an optimized combination of information from different detector components. The PF candidates are classified as photons, charged hadrons, neutral hadrons, electrons [27], or muons [28]. Additional quality criteria are imposed on electron and muon candidates. For example, more restrictive conditions are placed on the ECAL shower shape and on the ratio of energies deposited in the HCAL and ECAL for electron candidates, and on the matching of track segments between the silicon tracker and muon detector for muon candidates. The event primary vertex is taken to be the reconstructed vertex with the largest sum of charged-track p_{T}^2 values and is required to lie within 24 cm (2 cm) of the center of the detector in the direction along (perpendicular to) the beam axis. Charged tracks from extraneous pp interactions within the same or a nearby bunch crossing ("pileup") are removed [29]. The PF objects serve as input for jet reconstruction, based on the anti-k_{T} algorithm [30, 31] with a distance parameter of 0.4. Jet quality criteria as described in Ref. [32] are applied to eliminate, for example, spurious events caused by calorimeter noise. Contributions to an individual jet's p_{T} from pileup interactions are subtracted [33], and corrections are applied as a function of jet p_{T} and η to account for residual effects of nonuniform detector response [34]. Jets must have $p_{\mathrm{T}} > 30\,\mathrm{GeV}$.

The identification of b jets is performed by applying the combined secondary vertex algorithm (CSVv2) at the medium working point [35] to reconstructed jets. The b tagging efficiency is measured both in a data sample of multijet events with a reconstructed muon, and in a data sample of $\mathrm{t\bar{t}}$ events, with consistent results, and the probability to misidentify a light-flavor quark or gluon jet as a b jet in a data sample of inclusive multijet events, all as a function of jet p_{T} and η. The signal efficiency for b jets (misidentification probability for light-flavor quark or gluon jets) is approximately 55% (1.6%) for jets with $p_{\mathrm{T}} \approx 30\,\mathrm{GeV}$. The corresponding misidentification probability for a charm quark jet is estimated from simulation to be 12%.

Electrons and muons are required to be isolated in order to reduce background from events with bottom and charm quarks. The isolation criterion is based on the variable I, which is the scalar p_{T} sum of all PF charged hadrons, neutral hadrons, and photons within a cone of radius $R = \sqrt{(\Delta\phi)^2 + (\Delta\eta)^2}$ around the lepton direction, divided by the lepton p_{T}, where ϕ is the azimuthal angle. The sum excludes the lepton under consideration and is corrected for the contribution of pileup [29]. The cone radius is $R = 0.2\,(0.05)$ for lepton $p_{\mathrm{T}} \leq 50\,\mathrm{GeV}$

(>200 GeV), and $R = 10\,\text{GeV}/p_\text{T}$ for $50 \leq p_\text{T} \leq 200\,\text{GeV}$. The reason for the decrease in R with increasing lepton p_T is to account for the increased collimation of the lepton parent particle's decay products as the object's Lorentz boost increases. We require $I < 0.1$ (< 0.2) for electrons (muons).

Charged tracks not identified as an isolated electron or muon are also subjected to an isolation criterion. To be considered an isolated charged-particle track, the scalar sum of charged-track p_T values (excluding the track under consideration) in a cone of radius $R = 0.3$ around the track direction, divided by the track p_T, must be less than 0.2 if the track is identified by the PF procedure as an electron or muon, and less than 0.1 otherwise.

3 Event selection and search regions

The following requirements define the selection criteria for signal event candidates:

- $N_\text{jet} \geq 4$, where the jets must satisfy $|\eta| < 2.4$; we require at least four jets because of our focus on gluino pair production;
- $H_\text{T} > 500\,\text{GeV}$, where H_T is the scalar p_T sum of jets with $|\eta| < 2.4$;
- $H_\text{T}^\text{miss} > 200\,\text{GeV}$, where H_T^miss is the magnitude of $\vec{H}_\text{T}^\text{miss}$, the negative of the vector p_T sum of jets with $|\eta| < 5$; the η range is extended in this case so that $\vec{H}_\text{T}^\text{miss}$ better represents the total missing transverse momentum in an event;
- no identified, isolated electron or muon candidate with $p_\text{T} > 10\,\text{GeV}$; electron (muon) candidates are restricted to $|\eta| < 2.5$ (<2.4);
- no isolated charged-particle track with $|\eta| < 2.4$, $m_\text{T} < 100\,\text{GeV}$, and $p_\text{T} > 10\,\text{GeV}$ ($p_\text{T} > 5\,\text{GeV}$ if the track is identified as an electron or muon candidate by the PF algorithm), where m_T is the transverse mass [36] formed from the $\vec{p}_\text{T}^\text{miss}$ and isolated-track p_T vector, with $\vec{p}_\text{T}^\text{miss}$ the negative of the vector p_T sum of all PF objects;
- $\Delta\phi_{H_\text{T}^\text{miss},\text{j}_i} > 0.5$ (>0.3) for the two highest p_T jets j_1 and j_2 (the next two highest p_T jets j_3 and j_4), with $\Delta\phi_{H_\text{T}^\text{miss},\text{j}_i}$ the angle between $\vec{H}_\text{T}^\text{miss}$ and the p_T vector of jet j_i.

The isolated-track requirement eliminates events with a hadronically decaying τ lepton, as well as isolated electrons or muons in cases where the lepton is not identified; the m_T requirement restricts this veto to tracks consistent with a W boson decay in order to minimize the impact on signal efficiency. For all-hadronic events, $\vec{p}_\text{T}^\text{miss}$ and $\vec{H}_\text{T}^\text{miss}$ are similar, but $\vec{H}_\text{T}^\text{miss}$ is less susceptible to uncertainties in the modeling of soft energy deposits. We choose $\vec{p}_\text{T}^\text{miss}$ for the m_T calculation for consistency with previous practice. The $\Delta\phi_{H_\text{T}^\text{miss},\text{j}_i}$ requirements reduce the background from QCD multijet processes, for which $\vec{H}_\text{T}^\text{miss}$ is usually aligned along a jet direction.

The search is performed in the following exclusive intervals of the four search variables:

- N_jet: 4–6, 7–8, $\geq$9;
- $N_\text{b-jet}$: 0, 1, 2, $\geq$3;
- H_T: 500–800, 800–1200, $\geq$1200 GeV;
- H_T^miss: 200–500, 500–750, $\geq$750 GeV.

Bins with both $H_\text{T} < 800\,\text{GeV}$ and $H_\text{T}^\text{miss} > 750\,\text{GeV}$ are discarded because events with $H_\text{T}^\text{miss} \gtrsim H_\text{T}$ are very likely to be background. Additionally, for $500 < H_\text{T}^\text{miss} < 750\,\text{GeV}$, an expanded interval $500 < H_\text{T} < 1200\,\text{GeV}$ is used, and for $H_\text{T}^\text{miss} > 750\,\text{GeV}$ a single interval $H_\text{T} > 800\,\text{GeV}$, because of the low expected number of signal events at large H_T^miss. The six search intervals in

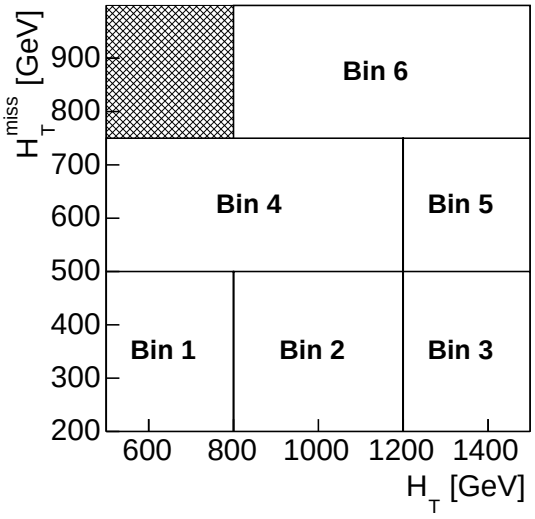

Figure 2: Schematic illustration of the search intervals in the H_T^{miss} versus H_T plane. Each of the six H_T and H_T^{miss} intervals is examined in three N_{jet} and four $N_{b\text{-}jet}$ bins for a total of 72 search regions.

the H_T^{miss} versus H_T plane are illustrated schematically in Fig. 2. The total number of search regions is 72.

A breakdown of the efficiency at different stages of the selection process for three representative signal models is given in Appendix A.

4 Event simulation

The background is mostly evaluated using data control regions, as described below (Section 5). Simulated samples of SM events are used to construct and validate the procedures and to estimate a few of the smaller background components. The MADGRAPH5_aMC@NLO 2.2.2 [37] event generator at leading order is used to simulate $t\bar{t}$, W+jets, Z+jets, γ+jets, and QCD multijet events. This same generator at next-to-leading (NLO) order is used to describe single top events in the *s* channel, events with dibosons (WW, ZZ, and WH production, etc., with H a Higgs boson), and rare processes ($t\bar{t}W$, $t\bar{t}Z$, and WWZ production, etc.), except WW events in which both W bosons decay leptonically are described with the POWHEG v1.0 [38–42] program at NLO. Single top events in the *t* and tW channels are also described with POWHEG at NLO. Simulation of the detector response is based on the GEANT4 [43] package. The simulated samples are normalized using the most accurate cross section calculations currently available [37, 41, 42, 44–52], generally with NLO or next-to-NLO accuracy.

Signal T1bbbb, T1tttt, T1qqqq, and T5qqqqVV events are generated for a range of gluino $m_{\tilde{g}}$ and LSP $m_{\tilde{\chi}_1^0}$ mass values, with $m_{\tilde{\chi}_1^0} < m_{\tilde{g}}$. For the T5qqqqVV model, the masses of the intermediate $\tilde{\chi}_2^0$ and $\tilde{\chi}_1^\pm$ states are taken to be the mean of $m_{\tilde{\chi}_1^0}$ and $m_{\tilde{g}}$. The signal samples are generated with the MADGRAPH5_aMC@NLO program at leading order, with up to two partons present in addition to the gluino pair. The decays of the gluino are described with a pure phase-space matrix element [53]. The signal production cross sections are computed [54–58] with NLO plus next-to-leading-logarithm (NLL) accuracy. To reduce computational requirements, the detector is modeled with the CMS fast simulation program [59, 60], which yields consistent results compared with the GEANT4-based simulation, except that we apply a correction of 1%

to account for differences in the efficiency of the jet quality requirements [32], and corrections of 3–10% to account for differences in the b jet tagging efficiency.

The NNPDF3.0LO [61] parton distribution functions (PDF) are used for the simulated samples generated at leading order, and the NNPDF3.0NLO [61] PDFs for the samples generated at NLO. All simulated samples use the PYTHIA 8.2 [53] program to describe parton showering and hadronization. To model the effects of pileup, the simulated events are generated with a nominal distribution of pp interactions per bunch crossing and then reweighted to match the corresponding distribution in data.

Table 1: Summary of systematic uncertainties that affect the signal event selection efficiency. The results are averaged over all search regions. The variations correspond to different signal models and choices of the gluino and LSP masses.

Item	Relative uncertainty (%)
Trigger efficiency	0.5–1.1
Pileup reweighting	0.1–0.5
Jet quality requirements	1.0
Renormalization and factorization scales	0.1–3.0
Initial-state radiation	0.02–10.0
Jet energy scale	0.5–4.0
Isolated lepton and track vetoes (T1tttt and T5qqqqVV only)	2.0
Total	1.5–11.0

We evaluate systematic uncertainties in the signal model predictions. Those that are relevant for the selection efficiency are listed in Table 1. The uncertainty associated with the renormalization and factorization scales is determined by varying each scale independently by factors of 2.0 and 0.5 [62, 63]. An uncertainty related to the modeling of initial-state radiation (ISR) is determined by comparing the simulated and measured p_T spectra of the system recoiling against the ISR jets in $t\bar{t}$ events, using the technique described in Ref. [64]. The two spectra are observed to agree. The statistical precision of the comparison is used to define an uncertainty of 15% (30%) for $400 < p_T < 600\,\text{GeV}$ ($p_T > 600\,\text{GeV}$), while no uncertainty is deemed necessary for $p_T < 400\,\text{GeV}$. The uncertainties associated with the renormalization and factorization scales, and with ISR, integrated over all search regions, typically lie below 0.1% but can be as large as 1–3%, and 3–10%, respectively, for $m_{\tilde{\chi}_1^0} \sim m_{\tilde{g}}$ (we use the notation $m_{\tilde{\chi}_1^0} \sim m_{\tilde{g}}$ to mean $m_{\tilde{\chi}_1^0} + 2m_X \approx m_{\tilde{g}}$, with m_X the bottom quark mass, the top quark mass, or the mass of the "V" boson, respectively, for the T1bbbb, T1tttt, and T5qqqqVV models; for the T1qqqq model, $m_{\tilde{\chi}_1^0} \sim m_{\tilde{g}}$ means $m_{\tilde{\chi}_1^0} \approx m_{\tilde{g}}$). The uncertainty associated with the jet energy scale is evaluated as a function of jet p_T and η. Note that the isolated lepton and track vetoes have a minimal impact on the T1bbbb and T1qqqq models because events in these models rarely contain an isolated lepton, and that the associated uncertainty is negligible ($\lesssim$0.1%).

We also evaluate systematic uncertainties in the signal predictions related to the b jet tagging and misidentification efficiencies and to the statistical uncertainties in the signal event samples. These sources of uncertainty do not affect the signal efficiency but can potentially alter the signal distribution shapes. Similarly, the sources of systematic uncertainty associated with the trigger efficiency, pileup reweighting, renormalization and factorization scales, ISR, and jet energy scale can affect the shapes of the signal distributions. These potential changes in shape, i.e., migration of events between search regions, are accounted for in the limit-setting procedure described in Section 6.

The systematic uncertainty in the determination of the integrated luminosity is 4.6%.

5 Background evaluation

In this section, we describe the evaluation of the background from SM processes. This evaluation relies on data control regions (CRs) selected using similar criteria to the search regions. Signal events may contribute to the CRs. The impact of this "signal contamination" on the final results is evaluated in the context of each individual SUSY model, as described in Section 6. However, the level of signal contamination is negligible for all CRs except those used to evaluate the top quark and W+jets background (Section 5.1), and is nonnegligible only for the T1tttt and T5qqqqVV models. The level of signal contamination for these nonnegligible cases is discussed in Sections 5.1.1 and 5.1.2.

5.1 Background from top quark and W+jets events

Background from SM $\mathrm{t\bar{t}}$, single top quark, and W+jets events arises when a W boson decays leptonically, yielding a neutrino (thus, genuine $H_{\mathrm{T}}^{\mathrm{miss}}$) and a non-vetoed charged lepton. The non-vetoed lepton can be an electron or muon (including from τ lepton decay) that does not satisfy the identification requirements of Section 3 (so-called "lost leptons"), or it can be a hadronically decaying τ lepton.

5.1.1 Lost-lepton background

Lost-lepton background can arise if an electron or muon lies outside the analysis acceptance, is not isolated, or is not reconstructed. The lost-lepton background is evaluated following the procedures established in Refs. [23, 65, 66]. Briefly, single-lepton CRs are selected by inverting the electron and muon vetoes. Each CR event is entered into one of the 72 search regions with a weight that represents the probability for a lost-lepton event to appear with the corresponding values of H_{T}, $H_{\mathrm{T}}^{\mathrm{miss}}$, N_{jet}, and $N_{\text{b-jet}}$.

The CRs are selected by requiring events to satisfy the criteria of Section 3 except exactly one isolated electron or muon must be present and the isolated-track veto is not applied. The transverse mass formed from the $\vec{p}_{\mathrm{T}}^{\,\mathrm{miss}}$ and lepton p_{T} vector is required to satisfy $m_{\mathrm{T}} < 100\,\mathrm{GeV}$: this requirement is effective at identifying SM events, which primarily arise from leptonic W boson decay, while reducing signal contamination. After applying this requirement, the fraction of CR events due to T1tttt (T5qqqqVV) signal contamination is generally negligible, viz., $\lesssim 0.1\%$, but it can be as high as around 30–40% (5–20%) for the largest values of N_{jet}, $N_{\text{b-jet}}$, H_{T}, and/or $H_{\mathrm{T}}^{\mathrm{miss}}$, depending on $m_{\tilde{\mathrm{g}}}$ and $m_{\tilde{\chi}_1^0}$. The weights, accounting for the probability for a lepton to be "lost", are determined from the $\mathrm{t\bar{t}}$, W+jets, single top quark, and rare process simulations through evaluation of the efficiency of the acceptance, reconstruction, and isolation requirements as a function of H_{T}, $H_{\mathrm{T}}^{\mathrm{miss}}$, N_{jet}, lepton p_{T}, and other kinematic variables. Since the efficiencies are parametrized in terms of kinematic and topological quantities, the method is insensitive to the specific mix of processes, i.e., it does not require the relative fractions of $\mathrm{t\bar{t}}$, single top, and W+jets events in the CRs to be the same as in the search regions (nonetheless, these fractions agree to within less than 1% in simulation). A correction derived from data is applied to the weights to account for the trigger efficiency, while corrections from simulation account for contamination due to nonprompt electrons, contamination due to dilepton events in which one of the leptons is lost, and the selection efficiency of the m_{T} requirement. Corresponding efficiencies are evaluated for dileptonic events in which both leptons are lost. This latter source of background is predicted to account for $<2\%$ of the total lost-lepton background. Finally, a correction is applied to account for the selection efficiency of the isolated-track veto.

The weighted distributions of the search variables, summed over the events in the CRs, define the lost-lepton background prediction. The procedure is performed separately for single-

electron and single-muon events. The two independent predictions yield consistent results and are averaged to obtain the final lost-lepton background prediction. The method is validated with a closure test, namely by determining the ability of the method, applied to simulated samples, to predict correctly the true number of background events. The results of the closure test are shown in the upper plot of Fig. 3. As a check, we repeated the closure test after varying the fractions of $\mathrm{t\bar{t}}$, single top, and W+jets events, with no discernible change in the outcome.

The dominant uncertainties in the lost-lepton background prediction are statistical, due to the limited number of CR events in the most sensitive search regions. As a systematic uncertainty, we take the larger of the observed nonclosure in Fig. 3 (upper plot) or the statistical uncertainty in the nonclosure, for each search region, where "nonclosure" refers to the difference between the solid points and histogram. Additional systematic uncertainties are assigned based on a comparison between data and simulation of the lepton reconstruction, lepton isolation, and isolated track veto efficiencies. Within the statistical precision, there are no such differences observed, and the statistical uncertainty in the respective comparison is assigned as a systematic uncertainty. Uncertainties in the acceptance associated with the PDFs, including those related to the renormalization and factorization scales, are evaluated by varying the PDF sets used to produce the simulated samples. These uncertainties are defined by the maximum deviations observed from 100 variations of the NNPDF3.0LO PDFs for $\mathrm{t\bar{t}}$ and W+jets events. The uncertainty in the jet energy correction is propagated to $\vec{p}_{\mathrm{T}}^{\,\mathrm{miss}}$, and the resulting change in the m_{T} selection efficiency is used to define a systematic uncertainty. Small systematic uncertainties related to the purity of the electron and muon CRs and to the statistical uncertainties in the simulated efficiencies are also evaluated.

5.1.2 Hadronically decaying τ lepton background

To evaluate the background due to W bosons that decay to a neutrino and a hadronically decaying τ lepton (τ_{h}), we employ a template method [23, 65, 66]. The τ_{h} background is determined from a single-muon CR, composed almost entirely of $\mathrm{t\bar{t}}$, single top quark, and W+jets events, selected using a trigger that requires $H_{\mathrm{T}} > 350\,\mathrm{GeV}$ and at least one muon candidate with $p_{\mathrm{T}} > 15\,\mathrm{GeV}$. The CR events are required to contain exactly one identified muon with $p_{\mathrm{T}} > 20\,\mathrm{GeV}$ and $|\eta| < 2.1$. Since μ+jets and τ_{h}+jets production arise from the same underlying process, the hadronic component of the events is expected to be the same aside from the response of the detector to a μ or τ_{h}. The muon p_{T} in the single-muon CR is smeared according to the response functions ("templates") derived from $\mathrm{t\bar{t}}$ and W+jets simulation. The templates express the expected visible-p_{T} distribution of a τ_{h} candidate as a function of the true τ-lepton p_{T} value, taken to be the measured muon p_{T}. The fraction of T1tttt (T5qqqqVV) events in the CR due to signal contamination is generally $\lesssim 0.1\%$, but can be as large as around 15–25% (4–8%) for the largest values of N_{jet}, $N_{\text{b-jet}}$, H_{T}, and/or $H_{\mathrm{T}}^{\mathrm{miss}}$, depending on $m_{\tilde{\mathrm{g}}}$ and $m_{\tilde{\chi}_1^0}$.

Following the smearing, the values of H_{T}, $H_{\mathrm{T}}^{\mathrm{miss}}$, N_{jet}, and $N_{\text{b-jet}}$ are calculated for the CR event, and the selection criteria of Section 3 are applied. The misidentification probability for a τ_{h} jet to be erroneously identified as a b jet is taken into account. Corrections are applied to account for the trigger efficiency, the acceptance and efficiency of the μ selection, and the ratio of branching fractions $BF(\mathrm{W} \to \tau_{\mathrm{h}}\nu)/BF(\mathrm{W} \to \mu\nu) = 0.65$ [67]. The resulting event yield provides the τ_{h} background estimate. The method is validated with a closure test, whose results are shown in the lower plot of Fig. 3. Systematic uncertainties are assigned based on the level of closure, as described for the lost-lepton background. Other systematic uncertainties are associated with the muon acceptance, the response functions, and the misidentification rate of τ_{h} jets as b jets. The dominant uncertainty, as for the lost-lepton background, arises from the limited number of events in the CR.

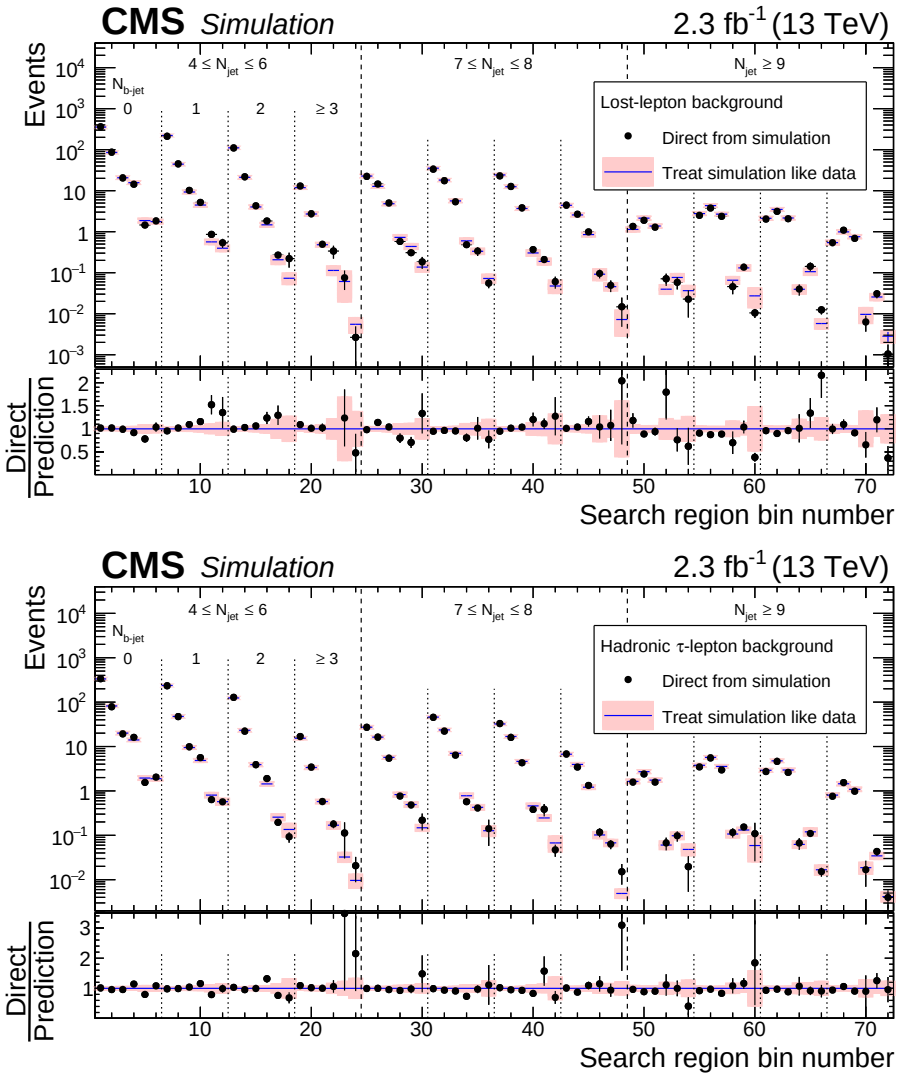

Figure 3: (upper plot) The lost-lepton background in the 72 search regions of the analysis as determined directly from $t\bar{t}$, single top quark, W+jets, diboson, and rare-event simulation (points, with statistical uncertainties) and as predicted by applying the lost-lepton background determination procedure to simulated electron and muon control samples (histograms, with statistical uncertainties). The lower panel shows the same results following division by the predicted value, where bins without markers have ratio values outside the scale of the plot. (lower plot) The corresponding simulated results for the background from hadronically decaying τ leptons. For both plots, the six results within each region delineated by dashed lines correspond sequentially to the six regions of H_T and H_T^{miss} indicated in Fig. 2.

5.2 Background from $Z \to \nu\bar{\nu}$ events

A straightforward method to evaluate the background from Z+jets events with $Z \to \nu\bar{\nu}$ consists of selecting Z+jets events with $Z \to \ell^+\ell^-$ (ℓ = e, μ), removing the ℓ^+ and ℓ^- to emulate the $Z \to \nu\bar{\nu}$ process, and applying the event selection criteria of Section 3. The resulting efficiency-corrected event yields can be directly translated into a prediction for the $Z \to \nu\bar{\nu}$ background through multiplication by the known ratio of branching fractions [67]. A limitation of this procedure is the small $Z \to \ell^+\ell^-$ branching fraction in relation to that for $Z \to \nu\bar{\nu}$.

An alternative approach is to exploit the similarity between Z boson radiation and the more copious radiation of photons by selecting γ+jets events, removing the photon from the event, and applying the selection criteria of Section 3. The γ+jets process differs from the Z+jets process because of threshold effects associated with the Z boson mass and because of the different couplings of Z bosons and photons to up- and down-type quarks. These differences are generally well understood and described adequately with simulation.

Our evaluation of the $Z \to \nu\bar{\nu}$ background utilizes both approaches. A γ+jets CR is selected using a trigger that requires $H_T > 500\,\text{GeV}$ and photon $p_T > 90\,\text{GeV}$. A Z+jets CR with $Z \to \ell^+\ell^-$ is selected using a trigger that requires $H_T > 350\,\text{GeV}$ and at least one electron or muon with $p_T > 15\,\text{GeV}$. Fits as described in Refs. [23] and [22] are used to extract the prompt-photon and Z boson yields, respectively. Because of current limitations in the simulations for the theoretical modeling of γ+jets versus Z+jets production with heavy flavor jets, we restrict the use of γ+jets events to the 18 search regions with $N_{\text{b-jet}} = 0$. The $Z \to \ell^+\ell^-$ sample, integrated over H_T and H_T^{miss} because of the limited statistical precision, is used to extrapolate the $N_{\text{b-jet}} = 0$ results to the $N_{\text{b-jet}} > 0$ search regions.

The γ+jets analysis is similar to that presented in Ref. [23]. We predict the number $N^{\text{pred}}_{Z\to\nu\bar{\nu}}$ of $Z(\to \nu\bar{\nu})$+jets events contributing to each $N_{\text{b-jet}} = 0$ search region from the number N^{data}_{γ} of events in the corresponding N_{jet}, H_T, and H_T^{miss} bin of the γ+jets CR:

$$N^{\text{pred}}_{Z\to\nu\bar{\nu}}\Big|_{N_{\text{b-jet}}=0} = \rho \mathcal{R}^{\text{sim}}_{Z\to\nu\bar{\nu}/\gamma} \beta^{\text{data}}_{\gamma} N^{\text{data}}_{\gamma}, \tag{1}$$

where $\beta^{\text{data}}_{\gamma}$ is the purity of the CR, determined from the fit [23] to data, and $\mathcal{R}^{\text{sim}}_{Z\to\nu\bar{\nu}/\gamma}$ the ratio from simulation ("sim") of the numbers of $Z(\to \nu\bar{\nu})$+jets events to γ+jets events, with the γ+jets term obtained from a leading-order MADGRAPH5_aMC@NLO calculation. Corrections are applied to account for efficiency differences between the data and simulation and for an angular cutoff in the simulation that controls the singularity associated with soft collinear radiative corrections. The factor ρ [23] in Eq. (1), defined as

$$\rho = \frac{\mathcal{R}^{\text{data}}_{Z\to\ell^+\ell^-/\gamma}}{\mathcal{R}^{\text{sim}}_{Z\to\ell^+\ell^-/\gamma}} = \frac{N^{\text{data}}_{Z\to\ell^+\ell^-}}{N^{\text{data}}_{\gamma}} \frac{N^{\text{sim}}_{\gamma}}{N^{\text{sim}}_{Z\to\ell^+\ell^-}}, \tag{2}$$

uses the $Z \to \ell^+\ell^-$ CR to account for potential differences in the $\mathcal{R}_{Z\to\nu\bar{\nu}/\gamma}$ factor between simulation and data, such as those expected due to missing higher-order terms in the γ+jets calculation, and is found to have a value of 0.92 (taken to be constant), with uncertainties, deduced from linear fits to projections onto each dimension, that vary with N_{jet}, H_T, and H_T^{miss} between 8 and 60%.

For search regions with $N_{\text{b-jet}} > 0$, the $Z \to \nu\bar{\nu}$ background estimate is

$$\left(N^{\text{pred}}_{Z\to\nu\bar{\nu}}\right)_{j,b,k} = \left(N^{\text{pred}}_{Z\to\nu\bar{\nu}}\right)_{j,0,k} \mathcal{F}_{j,b}; \tag{3}$$

$$\mathcal{F}_{j,b} = \left[\left(N^{\text{data}}_{Z\to\ell^+\ell^-}\beta^{\text{data}}_{\ell\ell}\right)_{0,b} / \left(N^{\text{data}}_{Z\to\ell^+\ell^-}\beta^{\text{data}}_{\ell\ell}\right)_{0,0}\right] \mathcal{J}_{j,b}; \tag{4}$$

$$\mathcal{J}_{j,b} = N^{\text{model}}_{j,b} / N^{\text{model}}_{0,b}, \tag{5}$$

where j, b, and k are bin indices (numbered from zero) for the N_{jet}, $N_{\text{b-jet}}$, and kinematic (i.e., H_{T} and $H_{\text{T}}^{\text{miss}}$) variables, respectively. For example, $j = 0$ ($b = 3$) corresponds to N_{jet} =4–6 ($N_{\text{b-jet}} \geq 3$), while $k = 0$ denotes "Bin 1" of Fig. 2. The first term on the right-hand side of Eq. (3) is obtained from Eq. (1). The $N_{\text{b-jet}}$ extrapolation factor $\mathcal{F}$ [Eq. (4)] is obtained from the fitted $Z \to \ell^+\ell^-$ yields, with data-derived corrections $\beta^{\text{data}}_{\ell\ell}$ to account for the $N_{\text{b-jet}}$-dependent purity. Other efficiencies cancel in the ratio. The dependence of the $N_{\text{b-jet}}$ shape of $\mathcal{F}$ on N_{jet} is described with the factor $\mathcal{J}$ [Eq. (5)], which is determined using a model estimate $N^{\text{model}}_{j,b}$ because of the limited statistical precision of the $Z \to \ell^+\ell^-$ data. The model uses the results of the $Z \to \ell^+\ell^-$ simulation for the central value of $\mathcal{J}$. Based on simulation studies, we determine corresponding upper and lower bounds to define a systematic uncertainty. As a lower bound on $\mathcal{J}$, we set $N^{\text{model}}_{j,b} = N^{\text{model}}_{0,b}$, i.e., $\mathcal{J}_{j,b} = 1$ in Eq. (4). In this limit $\mathcal{F}$ is independent of N_{jet}, corresponding to a factorization of the mechanisms to produce bottom quark jets and additional jets. As an upper bound, we take $N^{\text{model}}_{j,b} = \sum_{N_{\text{jet}}\in j, N_{\text{b-jet}}\in b} \mathcal{B}(N_{\text{b-jet}}|N_{\text{jet}}; p)$, where $\mathcal{B}$ is a binomial distribution, with p the probability for a jet to be tagged as a b jet. In both simulation and data we find p to be independent of N_{jet}. This binomial behavior would be expected should all tagged b jets be erroneous, i.e., not initiated by b quarks, or should the production of quarks in the hadron shower not depend on flavor except via a scale factor that is absorbed into the empirical factor p. With respect to a systematic uncertainty, the factorization and binomial extrapolations represent opposite extremes. The binomial assumption is validated in simulation; the result $p = 0.062 \pm 0.007$ is obtained from a fit to the data, of which $\simeq$0.02 is attributable to light-parton or charm quark jets erroneously identified as b jets. The resulting systematic uncertainties in $\mathcal{J}$ range from a few percent to $\approx$60%, depending on N_{jet} and $N_{\text{b-jet}}$.

A closure test of the method is presented in Fig. 4. The shaded bands represent the systematic uncertainty (10–20%, depending on $N_{\text{b-jet}}$) arising from our treatment of $\mathcal{F}$ as independent of the kinematic parameters, combined with the statistical uncertainty of the $Z(\to \ell^+\ell^-)$+jets simulation.

Rare processes such as $t\bar{t}Z$ and V(V)Z (V = W or Z) production can contribute to the background. We add the expectations for these processes, obtained from simulation, to the background predicted from the procedure described above. Note that processes with a Z boson and a $Z \to \gamma$ counterpart are already accounted for in N^{data}_{γ} and largely cancel in the $\mathcal{R}_{Z\to\nu\bar{\nu}/\gamma}$ ratio. For search regions with $N_{\text{b-jet}} \geq 2$, the contribution of $t\bar{t}Z$ events is found to be comparable to that from Z+jets events, with an uncertainty of $\approx$50%, consistent with the rate and uncertainty for $t\bar{t}Z$ events found in Ref. [68].

Besides the uncertainty related to the $N_{\text{b-jet}}$ extrapolation, discussed above, systematic uncertainties associated with the statistical precision of the simulation, the photon reconstruction efficiency, the photon and dilepton purities, and the $\rho\mathcal{R}^{\text{sim}}_{Z\to\nu\bar{\nu}/\gamma}$ term are evaluated. Of these, the $\rho\mathcal{R}^{\text{sim}}_{Z\to\nu\bar{\nu}/\gamma}$ term (10–60%) dominates the overall uncertainty except in the highest (N_{jet}, $N_{\text{b-jet}}$) search regions where the overall uncertainty is dominated by the statistical precision of the simulation (70–110%) and by the uncertainty in the $Z \to \ell^+\ell^-$ purity (40%). The underlying source of the leading systematic uncertainties is the limited number of events in the CR.

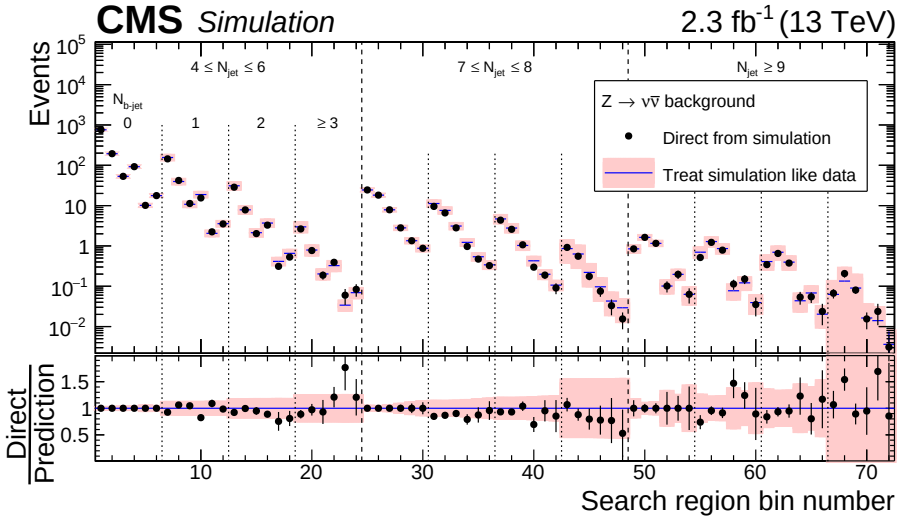

Figure 4: The $Z \to \nu\bar{\nu}$ background in the 72 search regions of the analysis as determined directly from $Z(\to \nu\bar{\nu})$+jets and $t\bar{t}Z$ simulation (points), and as predicted by applying the $Z \to \nu\bar{\nu}$ background determination procedure to statistically independent $Z(\to \ell^+\ell^-)$+jets simulated event samples (histogram). For bins corresponding to $N_{\text{b-jet}} = 0$, the agreement is exact by construction. The lower panel shows the ratio between the true and predicted yields. For both the upper and lower panels, the shaded regions indicate the quadrature sum of the systematic uncertainty associated with the dependence of $\mathcal{F}$ on the kinematic parameters (H_{T} and $H_{\text{T}}^{\text{miss}}$) and the statistical uncertainty of the simulated sample. The labeling of the search regions is the same as in Fig. 3.

5.3 Background from QCD multijet events

To evaluate the background associated with QCD multijet production, we select a QCD dominated CR by inverting the $\Delta\phi_{H_{\text{T}}^{\text{miss}},j_i}$ requirements, i.e., by requiring at least one of the four highest p_{T} jets in an event to fail the respective $\Delta\phi_{H_{\text{T}}^{\text{miss}},j_i}$ selection criterion listed in Section 3. The resulting sample is called the "low-$\Delta\phi$" CR. The QCD background in each search region is given by the product of the observed event yield in the corresponding region of the low-$\Delta\phi$ CR multiplied by a factor R^{QCD} expressing the ratio of the expected QCD multijet background in the respective signal and low-$\Delta\phi$ regions, taking into account the contributions from non-QCD SM processes. The non-QCD SM contributions to the low-$\Delta\phi$ CR, which correspond to around 14% of the events in this CR, are evaluated using the techniques described above for the top quark, W+jets, and Z+jets backgrounds, except with the inverted $\Delta\phi_{H_{\text{T}}^{\text{miss}},j_i}$ requirements. The R^{QCD} terms are determined primarily from data, as described below. The procedure is analogous to that used in Refs. [22, 69] to evaluate the QCD multijet background.

The R^{QCD} factor increases with N_{jet} but is found empirically to have a negligible dependence on $N_{\text{b-jet}}$ for a given N_{jet} value. We therefore divide the $4 \leq N_{\text{jet}} \leq 6$ search region into three exclusive bins: $N_{\text{jet}} = 4$, 5, and 6. Once this is done, there is no dependence of R^{QCD} on $N_{\text{b-jet}}$. Similarly, we divide the $200 \leq H_{\text{T}}^{\text{miss}} \leq 500\,\text{GeV}$ search region into two bins: $200 < H_{\text{T}}^{\text{miss}} < 300\,\text{GeV}$ and $300 < H_{\text{T}}^{\text{miss}} < 500\,\text{GeV}$; the first of these two bins is enhanced in QCD background events, both in the low-$\Delta\phi$ and signal samples. The H_{T}, $H_{\text{T}}^{\text{miss}}$, and N_{jet} dependence of R^{QCD} is modeled as:

$$R^{\text{QCD}}_{i,j,k} = K^{\text{data}}_{H_{\text{T}},i} S^{\text{sim}}_{H_{\text{T}}^{\text{miss}},j} S^{\text{data}}_{N_{\text{jet}},k}, \tag{6}$$

where i, j, and k are bin indices. The $K^{\text{data}}_{H_{\text{T}},i}$ term is the ratio of the expected number of QCD

multijet events in the search region to that in the low-$\Delta\phi$ region for H_T bin i in the first H_T^{miss} and N_{jet} bins. The $S^{sim}_{H_T^{miss},j}$ term represents a correction for H_T^{miss} bin j with respect to the first H_T^{miss} bin, and the $S^{data}_{N_{jet},k}$ term a correction for N_{jet} bin k with respect to the first N_{jet} bin. The $K^{data}_{H_T,i}$ and $S^{data}_{N_{jet},k}$ terms are determined from a fit to data in the $200 < H_T^{miss} < 300$ GeV bin, with the non-QCD SM background taken into account. The $S^{sim}_{H_T^{miss},j}$ terms are taken from the QCD multijet simulation. Based on studies of the differing contributions of events in which the jet with the largest p_T mismeasurement is or is not amongst the four highest p_T jets, uncertainties of 50, 100, and 100% are assigned to the H_T^{miss} 300–500, 500–750, and ≥ 750 GeV bins, respectively, to account for potential differences between data and simulation in the $S_{H_T^{miss},j}$ factors. Weighted results for R^{QCD} are calculated when recombining the H_T^{miss} and N_{jet} results to correspond to the nominal search regions. Figure 5 presents closure test results for the method.

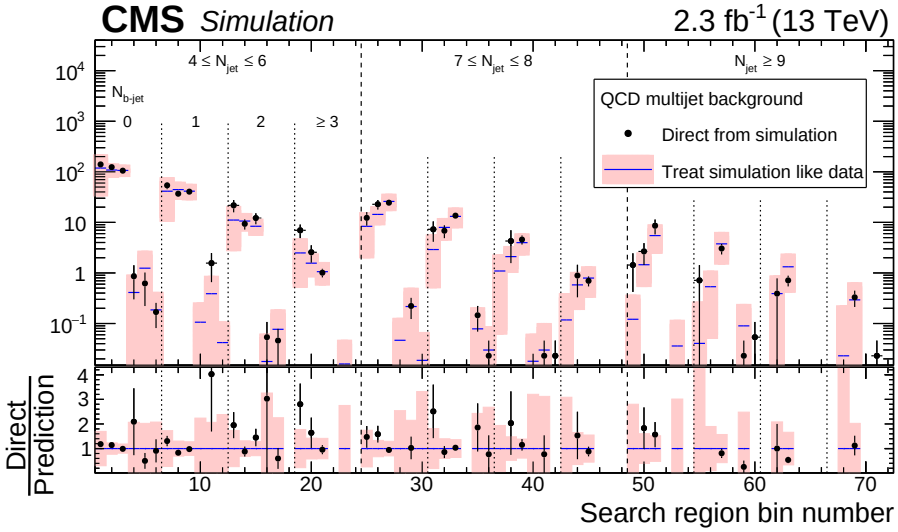

Figure 5: The QCD multijet background in the 72 search regions of the analysis as determined directly from QCD multijet simulation (points, with statistical uncertainties) and as predicted by applying the QCD multijet background determination procedure to simulated event samples (histograms, with statistical and systematic uncertainties added in quadrature). The lower panel shows the same results following division by the predicted value. The labeling of the search regions is the same as in Fig. 3. Bins without markers have no events in the control regions. No result is given in the lower panel if the value of the prediction is zero.

For the lowest H_T^{miss} search region, the uncertainty in the prediction of the QCD multijet background is dominated by the uncertainties in $K^{data}_{H_T,i}$ and $S^{data}_{N_{jet},k}$, which themselves are mostly due to uncertainties in the non-QCD SM background in the search regions. For the two higher H_T^{miss} search regions, the uncertainty in $S^{sim}_{H_T^{miss},j}$ and the limited statistical precision of the low-$\Delta\phi$ CR dominate the uncertainty. The uncertainties related to potential nonclosure (Fig. 5) are either small in comparison or statistical in nature and are not considered.

6 Results and interpretation

The observed numbers of events in the 72 search regions are shown in Fig. 6 in comparison to the summed predictions for the SM backgrounds, with numerical values tabulated in Appendix B. The predicted background is observed to be statistically compatible with the data for all 72 regions. Therefore, we do not observe evidence for new physics.

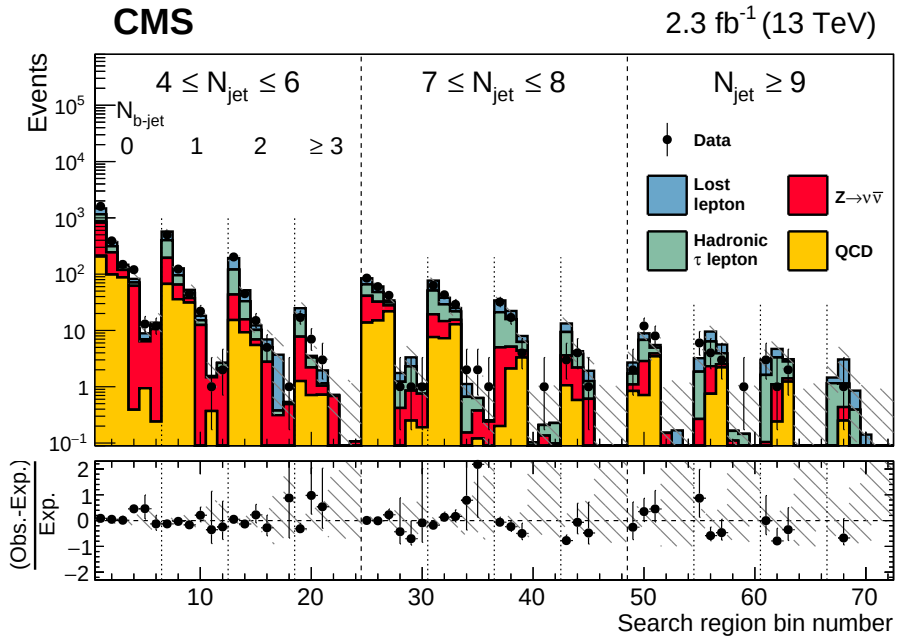

Figure 6: Observed numbers of events and corresponding prefit SM background predictions in the 72 search regions of the analysis, with fractional differences shown in the lower panel. The shaded regions indicate the total uncertainties in the background predictions. The labeling of the search regions is the same as in Fig. 3.

Figure 7 presents one-dimensional projections of the results in $H_{\mathrm{T}}^{\mathrm{miss}}$ or H_{T} after criteria are imposed, as indicated in the legends, to select intervals of the search region parameter space particularly sensitive to the T1bbbb, T1tttt, T1qqqq, or T5qqqqVV scenario. In each case, example distributions are shown for two signal scenarios not excluded by our Run 1 studies [22, 23]. These scenarios, one with $m_{\tilde{\mathrm{g}}} \gg m_{\tilde{\chi}_1^0}$ and one with $m_{\tilde{\chi}_1^0} \sim m_{\tilde{\mathrm{g}}}$, lie well within the parameter space excluded by the present analysis (see below).

A likelihood fit to data is used to set limits on the production cross sections of the signal scenarios. The fitted parameters are the SUSY signal strength, the yields of the four background classes indicated in Fig. 6, and various nuisance parameters. The limits are determined as a function of $m_{\tilde{\chi}_1^0}$ and $m_{\tilde{\mathrm{g}}}$. The likelihood function is the product of Poisson probability density functions, one for each search region, and constraint terms that account for uncertainties in the background predictions and signal yields. These uncertainties are treated as nuisance parameters with log-normal probability density functions. Correlations are taken into account where appropriate. The signal model uncertainties associated with the renormalization and factorization scales, ISR, the jet energy scale, the b jet tagging, and the statistical fluctuations vary substantially with the event kinematics and are evaluated as a function of $m_{\tilde{\chi}_1^0}$ and $m_{\tilde{\mathrm{g}}}$. The test statistic is $q_\mu = -2\ln\left(\mathcal{L}_\mu/\mathcal{L}_{\mathrm{max}}\right)$, where $\mathcal{L}_{\mathrm{max}}$ is the maximum likelihood determined by allowing all parameters including the SUSY signal strength μ to vary, and $\mathcal{L}_\mu$ is the maximum likelihood for a fixed signal strength. To set limits, we use asymptotic results for the test statistic [70] and the $\mathrm{CL_s}$ method described in Refs. [71, 72]. More details are provided in Refs. [15, 73].

We proceed to evaluate 95% confidence level (CL) upper limits on the signal cross sections. The NLO+NLL cross section is used as a reference to evaluate corresponding 95% CL exclusion curves. In addition to the observed limits, expected limits are derived by evaluating the expected Poisson fluctuations around the predicted numbers of background events when eval-

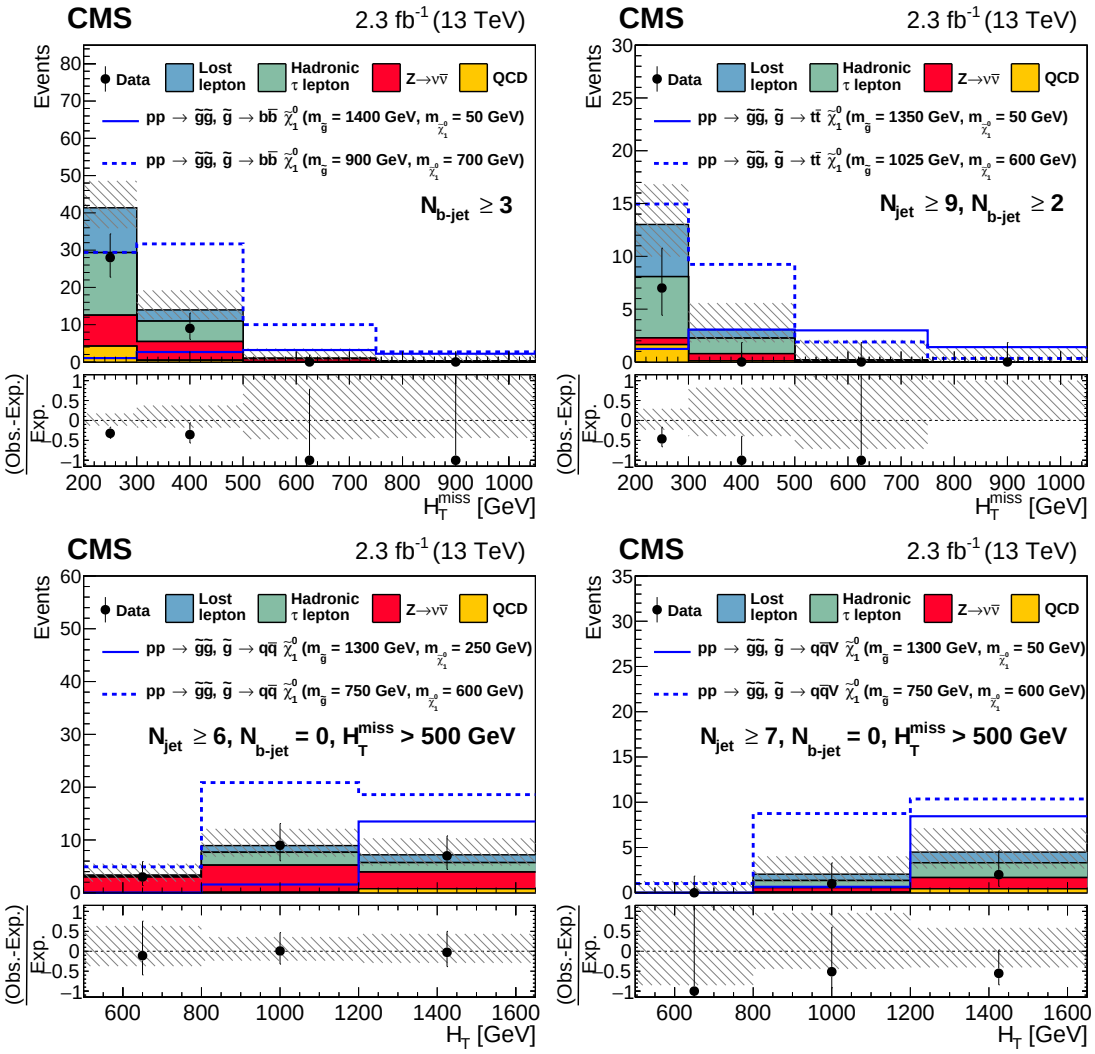
CMS
2.3 fb-1 (13 TeV)
Data
Lost lepton
Hadronic τ lepton
Z→νν̄
QCD
pp → g̃g̃, g̃ → bb̄ χ̃10 (mg̃ = 1400 GeV, mχ̃10 = 50 GeV)
pp → g̃g̃, g̃ → bb̄ χ̃10 (mg̃ = 900 GeV, mχ̃10 = 700 GeV)
Nb-jet ≥ 3
Events
(Obs.-Exp.)/Exp.
HTmiss [GeV]
CMS
2.3 fb-1 (13 TeV)
pp → g̃g̃, g̃ → tt̄ χ̃10 (mg̃ = 1350 GeV, mχ̃10 = 50 GeV)
pp → g̃g̃, g̃ → tt̄ χ̃10 (mg̃ = 1025 GeV, mχ̃10 = 600 GeV)
Njet ≥ 9, Nb-jet ≥ 2
CMS
2.3 fb-1 (13 TeV)
pp → g̃g̃, g̃ → qq̄ χ̃10 (mg̃ = 1300 GeV, mχ̃10 = 250 GeV)
pp → g̃g̃, g̃ → qq̄ χ̃10 (mg̃ = 750 GeV, mχ̃10 = 600 GeV)
Njet ≥ 6, Nb-jet = 0, HTmiss > 500 GeV
HT [GeV]
CMS
2.3 fb-1 (13 TeV)
pp → g̃g̃, g̃ → qq̄V χ̃10 (mg̃ = 1300 GeV, mχ̃10 = 50 GeV)
pp → g̃g̃, g̃ → qq̄V χ̃10 (mg̃ = 750 GeV, mχ̃10 = 600 GeV)
Njet ≥ 7, Nb-jet = 0, HTmiss > 500 GeV

Figure 7: Observed numbers of events and corresponding SM background predictions for intervals of the search region parameter space particularly sensitive to the (upper left) T1bbbb, (upper right) T1tttt, (lower left) T1qqqq, and (lower right) T5qqqqVV scenarios. The selection requirements are given in the figure legends. The hatched regions indicate the total uncertainties in the background predictions. The (unstacked) results for two example signal scenarios are shown in each instance, one with $m_{\tilde{g}} \gg m_{\tilde{\chi}^0_1}$ and the other with $m_{\tilde{\chi}^0_1} \sim m_{\tilde{g}}$. Note that for purposes of presentation, the four-bin scheme discussed in Section 5.3 is used for the H_T^{miss} variable. For the T1tttt model, the rightmost bin contains both zero predicted background events and zero observed events.

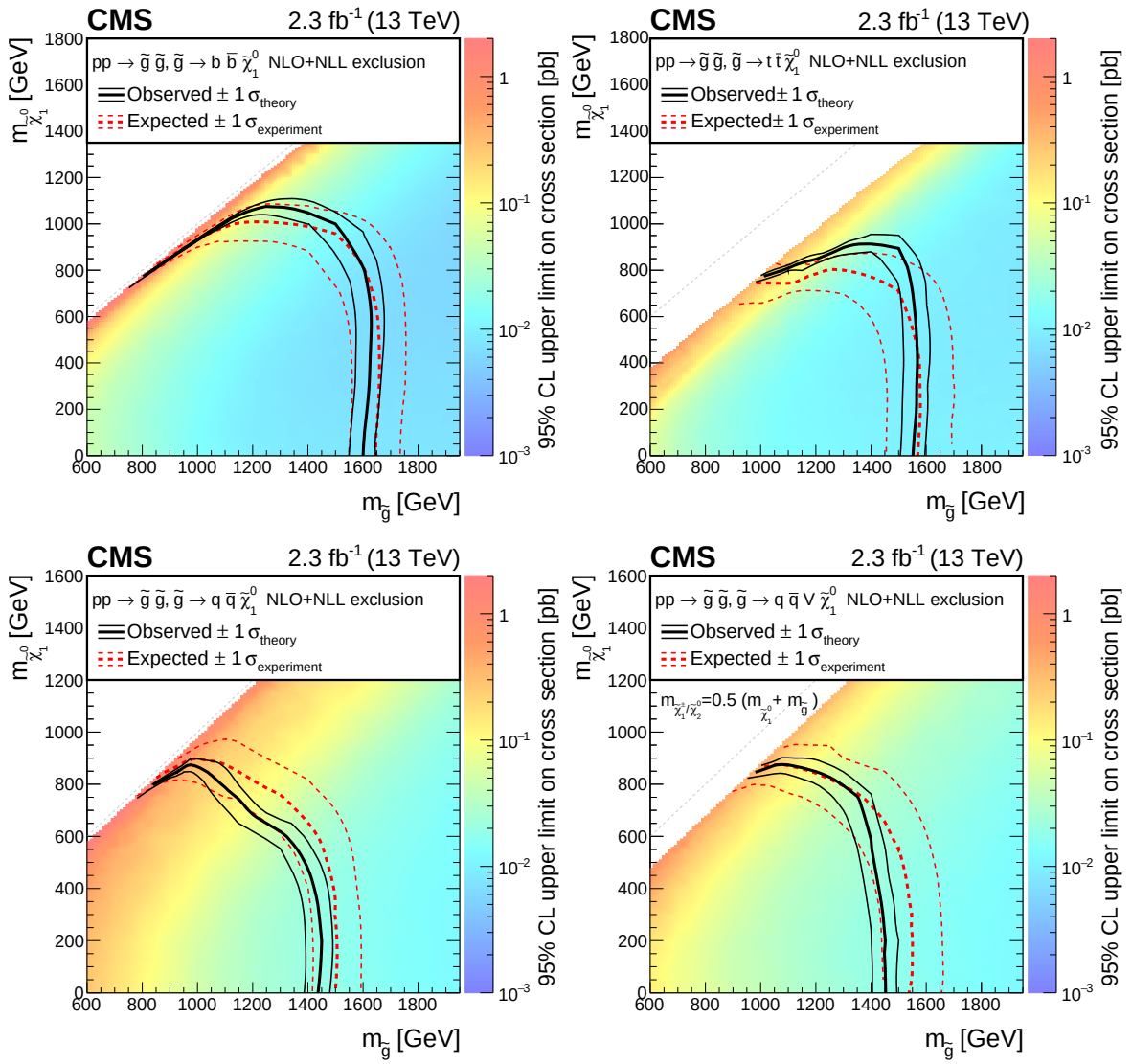
CMS
2.3 fb-1 (13 TeV)
pp → g̃ g̃, g̃ → b b̄ χ̃10 NLO+NLL exclusion
Observed ± 1 σtheory
Expected ± 1 σexperiment
pp → g̃ g̃, g̃ → t t̄ χ̃10 NLO+NLL exclusion
Observed ± 1 σtheory
Expected ± 1 σexperiment
pp → g̃ g̃, g̃ → q q̄ χ̃10 NLO+NLL exclusion
Observed ± 1 σtheory
Expected ± 1 σexperiment
pp → g̃ g̃, g̃ → q q̄ V χ̃10 NLO+NLL exclusion
Observed ± 1 σtheory
Expected ± 1 σexperiment
mχ̃1±/χ̃20=0.5 (mχ̃10+ mg̃)
mχ̃10 [GeV]
mg̃ [GeV]
95% CL upper limit on cross section [pb]

Figure 8: The 95% CL upper limits on the production cross sections for the (upper left) T1bbbb, (upper right) T1tttt, (lower left) T1qqqq, and (lower right) T5qqqqVV simplified models of supersymmetry, shown as a function of the gluino and LSP masses $m_{\tilde{g}}$ and $m_{\tilde{\chi}_1^0}$. For the T5qqqqVV model, the masses of the intermediate $\tilde{\chi}_2^0$ and $\tilde{\chi}_1^\pm$ states are taken to be the mean of $m_{\tilde{\chi}_1^0}$ and $m_{\tilde{g}}$. The solid (black) curves show the observed exclusion contours assuming the NLO+NLL cross sections [54–58], with the corresponding ± 1 standard deviation uncertainties [74]. The dashed (red) curves present the expected limits with ± 1 standard deviation experimental uncertainties. The dashed (grey) lines indicate the $m_{\tilde{\chi}_1^0} = m_{\tilde{g}}$ diagonal.

uating the test statistic. The potential contributions of signal events to the control regions are taken into account. Specifically, the number of events in each CR is corrected to include the predicted number of signal events, in the context of the model being examined, to derive the total effective number of background events expected in each search region. This total effective background is used when determining the limits.

The results are shown in Fig. 8. For a massless LSP, we exclude gluinos with masses below 1600, 1550, 1440, and 1450 GeV, respectively, for the T1bbbb, T1tttt, T1qqqq, and T5qqqqVV scenarios. These results significantly extend those we obtained at $\sqrt{s} = 8$ TeV, for which the corresponding limits are around 1150 GeV [22, 23] for the three T1 models and 1280 GeV [23] for the T5 model.

7 Summary

A search is presented for an anomalously high rate of events with four or more jets, no identified isolated electron or muon or isolated charged track, large scalar sum H_T of jet transverse momenta, and large missing transverse momentum, where this latter quantity is measured with the variable H_T^{miss}, the magnitude of the vector sum of jet transverse momenta. The search is based on a sample of proton-proton collision data collected at $\sqrt{s} = 13$ TeV with the CMS detector at the CERN LHC in 2015, corresponding to an integrated luminosity of 2.3 fb^{-1}. The principal standard model backgrounds, from events with top quarks, W bosons and jets, Z bosons and jets, and QCD multijet production, are evaluated using control samples in the data. The study is performed in the framework of a global likelihood fit in which the observed numbers of events in 72 exclusive bins in a four-dimensional array of H_T^{miss}, the number of jets, the number of tagged bottom quark jets, and H_T, are compared to the standard model predictions. The standard model background estimates are found to agree with the observed numbers of events within the uncertainties. The results are interpreted with simplified models that, in the context of supersymmetry, correspond to gluino pair production followed by the decay of each gluino to an undetected lightest-supersymmetric-particle (LSP) neutralino $\widetilde{\chi}_1^0$ and to a bottom quark-antiquark pair (T1bbbb model), a top quark-antiquark pair (T1tttt model), or a light-flavored quark-antiquark pair (T1qqqq model). We also consider a scenario corresponding to gluino pair production followed by the decay of each gluino to a light-flavored quark-antiquark pair and to either a next-to-lightest neutralino $\widetilde{\chi}_2^0$ or a lightest chargino $\widetilde{\chi}_1^\pm$, with $\widetilde{\chi}_2^0 \to Z\widetilde{\chi}_1^0$ or $\widetilde{\chi}_1^\pm \to W^\pm\widetilde{\chi}_1^0$ (T5qqqqVV model). Using the NLO+NLL production cross section as a reference, and for a massless LSP, we exclude gluinos with masses below 1600, 1550, 1440, and 1450 GeV for the four scenarios, respectively, significantly extending the limits from previous searches.

Acknowledgments

We congratulate our colleagues in the CERN accelerator departments for the excellent performance of the LHC and thank the technical and administrative staffs at CERN and at other CMS institutes for their contributions to the success of the CMS effort. In addition, we gratefully acknowledge the computing centers and personnel of the Worldwide LHC Computing Grid for delivering so effectively the computing infrastructure essential to our analyses. Finally, we acknowledge the enduring support for the construction and operation of the LHC and the CMS detector provided by the following funding agencies: BMWFW and FWF (Austria); FNRS and FWO (Belgium); CNPq, CAPES, FAPERJ, and FAPESP (Brazil); MES (Bulgaria); CERN; CAS, MoST, and NSFC (China); COLCIENCIAS (Colombia); MSES and CSF (Croatia); RPF (Cyprus); MoER, ERC IUT and ERDF (Estonia); Academy of Finland, MEC, and HIP (Finland); CEA and

CNRS/IN2P3 (France); BMBF, DFG, and HGF (Germany); GSRT (Greece); OTKA and NIH (Hungary); DAE and DST (India); IPM (Iran); SFI (Ireland); INFN (Italy); MSIP and NRF (Republic of Korea); LAS (Lithuania); MOE and UM (Malaysia); CINVESTAV, CONACYT, SEP, and UASLP-FAI (Mexico); MBIE (New Zealand); PAEC (Pakistan); MSHE and NSC (Poland); FCT (Portugal); JINR (Dubna); MON, RosAtom, RAS and RFBR (Russia); MESTD (Serbia); SEIDI and CPAN (Spain); Swiss Funding Agencies (Switzerland); MST (Taipei); ThEPCenter, IPST, STAR and NSTDA (Thailand); TUBITAK and TAEK (Turkey); NASU and SFFR (Ukraine); STFC (United Kingdom); DOE and NSF (USA).

Individuals have received support from the Marie-Curie program and the European Research Council and EPLANET (European Union); the Leventis Foundation; the A. P. Sloan Foundation; the Alexander von Humboldt Foundation; the Belgian Federal Science Policy Office; the Fonds pour la Formation à la Recherche dans l'Industrie et dans l'Agriculture (FRIA-Belgium); the Agentschap voor Innovatie door Wetenschap en Technologie (IWT-Belgium); the Ministry of Education, Youth and Sports (MEYS) of the Czech Republic; the Council of Science and Industrial Research, India; the HOMING PLUS program of the Foundation for Polish Science, cofinanced from European Union, Regional Development Fund; the OPUS program of the National Science Center (Poland); the Compagnia di San Paolo (Torino); MIUR project 20108T4XTM (Italy); the Thalis and Aristeia programmes cofinanced by EU-ESF and the Greek NSRF; the National Priorities Research Program by Qatar National Research Fund; the Rachadapisek Sompot Fund for Postdoctoral Fellowship, Chulalongkorn University (Thailand); the Chulalongkorn Academic into Its 2nd Century Project Advancement Project (Thailand); and the Welch Foundation, contract C-1845.

References

[1] P. Ramond, "Dual theory for free fermions", *Phys. Rev. D* **3** (1971) 2415, doi:10.1103/PhysRevD.3.2415.

[2] Y. A. Golfand and E. P. Likhtman, "Extension of the algebra of Poincaré group generators and violation of P invariance", *JETP Lett.* **13** (1971) 323.

[3] A. Neveu and J. H. Schwarz, "Factorizable dual model of pions", *Nucl. Phys. B* **31** (1971) 86, doi:10.1016/0550-3213(71)90448-2.

[4] D. V. Volkov and V. P. Akulov, "Possible universal neutrino interaction", *JETP Lett.* **16** (1972) 438.

[5] J. Wess and B. Zumino, "A Lagrangian model invariant under supergauge transformations", *Phys. Lett. B* **49** (1974) 52, doi:10.1016/0370-2693(74)90578-4.

[6] J. Wess and B. Zumino, "Supergauge transformations in four dimensions", *Nucl. Phys. B* **70** (1974) 39, doi:10.1016/0550-3213(74)90355-1.

[7] P. Fayet, "Supergauge invariant extension of the Higgs mechanism and a model for the electron and its neutrino", *Nucl. Phys. B* **90** (1975) 104, doi:10.1016/0550-3213(75)90636-7.

[8] H. P. Nilles, "Supersymmetry, supergravity and particle physics", *Phys. Rep.* **110** (1984) 1, doi:10.1016/0370-1573(84)90008-5.

[9] R. Barbieri and G. F. Giudice, "Upper Bounds on Supersymmetric Particle Masses", *Nucl. Phys. B* **306** (1988) 63, doi:10.1016/0550-3213(88)90171-X.

[10] S. Dimopoulos and G. F. Giudice, "Naturalness constraints in supersymmetric theories with nonuniversal soft terms", *Phys. Lett. B* **357** (1995) 573, doi:10.1016/0370-2693(95)00961-J, arXiv:hep-ph/9507282.

[11] R. Barbieri and D. Pappadopulo, "S-particles at their naturalness limits", *JHEP* **10** (2009) 061, doi:10.1088/1126-6708/2009/10/061, arXiv:0906.4546.

[12] M. Papucci, J. T. Ruderman, and A. Weiler, "Natural SUSY endures", *JHEP* **09** (2012) 035, doi:10.1007/JHEP09(2012)035, arXiv:1110.6926.

[13] G. R. Farrar and P. Fayet, "Phenomenology of the production, decay, and detection of new hadronic states associated with supersymmetry", *Phys. Lett. B* **76** (1978) 575, doi:10.1016/0370-2693(78)90858-4.

[14] ATLAS Collaboration, "Summary of the searches for squarks and gluinos using $\sqrt{s} = 8$ TeV pp collisions with the ATLAS experiment at the LHC", *JHEP* **10** (2015) 054, doi:10.1007/JHEP10(2015)054, arXiv:1507.05525.

[15] CMS Collaboration, "Searches for supersymmetry using the M_{T2} variable in hadronic events produced in pp collisions at 8 TeV", *JHEP* **05** (2015) 078, doi:10.1007/JHEP05(2015)078, arXiv:1502.04358.

[16] CMS Collaboration, "Search for supersymmetry using razor variables in events with b-tagged jets in pp collisions at $\sqrt{s} = 8$ TeV", *Phys. Rev. D* **91** (2015) 052018, doi:10.1103/PhysRevD.91.052018, arXiv:1502.00300.

[17] N. Arkani-Hamed et al., "MARMOSET: The path from LHC data to the new standard model via on-shell effective theories", (2007). arXiv:hep-ph/0703088.

[18] J. Alwall, P. Schuster, and N. Toro, "Simplified models for a first characterization of new physics at the LHC", *Phys. Rev. D* **79** (2009) 075020, doi:10.1103/PhysRevD.79.075020, arXiv:0810.3921.

[19] J. Alwall, M.-P. Le, M. Lisanti, and J. G. Wacker, "Model-independent jets plus missing energy searches", *Phys. Rev. D* **79** (2009) 015005, doi:10.1103/PhysRevD.79.015005, arXiv:0809.3264.

[20] D. Alves et al., "Simplified models for LHC new physics searches", *J. Phys. G* **39** (2012) 105005, doi:10.1088/0954-3899/39/10/105005, arXiv:1105.2838.

[21] CMS Collaboration, "Interpretation of searches for supersymmetry with simplified models", *Phys. Rev. D* **88** (2013) 052017, doi:10.1103/PhysRevD.88.052017, arXiv:1301.2175.

[22] CMS Collaboration, "Search for gluino mediated bottom- and top-squark production in multijet final states in pp collisions at 8 TeV", *Phys. Lett. B* **725** (2013) 243, doi:10.1016/j.physletb.2013.06.058, arXiv:1305.2390.

[23] CMS Collaboration, "Search for new physics in the multijet and missing transverse momentum final state in proton-proton collisions at $\sqrt{s} = 8$ TeV", *JHEP* **06** (2014) 055, doi:10.1007/JHEP06(2014)055, arXiv:1402.4770.

[24] CMS Collaboration, "The CMS experiment at the CERN LHC", *JINST* **3** (2008) S08004, doi:10.1088/1748-0221/3/08/S08004.

[25] CMS Collaboration, "Particle flow event reconstruction in CMS and performance for jets, taus and $E_{\mathrm{T}}^{\mathrm{miss}}$", CMS Physics Analysis Summary CMS-PAS-PFT-09-001, CERN, 2009.

[26] CMS Collaboration, "Commissioning of the particle-flow event reconstruction with the first LHC collisions recorded in the CMS detector", CMS Physics Analysis Summary CMS-PAS-PFT-10-001, CERN, 2010.

[27] CMS Collaboration, "Performance of electron reconstruction and selection with the CMS detector in proton-proton collisions at $\sqrt{s} = 8$ TeV", *JINST* **10** (2015) P06005, doi:10.1088/1748-0221/10/06/P06005, arXiv:1502.02701.

[28] CMS Collaboration, "The performance of the CMS muon detector in proton-proton collisions at $\sqrt{s} = 7$ TeV at the LHC", *JINST* **8** (2013) P11002, doi:10.1088/1748-0221/8/11/P11002, arXiv:1306.6905.

[29] CMS Collaboration, "Study of pileup removal algorithms for jets", CMS Physics Analysis Summary CMS-PAS-JME-14-001, CERN, 2014.

[30] M. Cacciari, G. P. Salam, and G. Soyez, "The Anti-k_t jet clustering algorithm", *JHEP* **04** (2008) 063, doi:10.1088/1126-6708/2008/04/063, arXiv:0802.1189.

[31] M. Cacciari, G. P. Salam, and G. Soyez, "FastJet user manual", *Eur. Phys. J. C* **72** (2012) 1896, doi:10.1140/epjc/s10052-012-1896-2, arXiv:1111.6097.

[32] CMS Collaboration, "Jet performance in pp collisions at $\sqrt{s} = 7$ TeV", CMS Physics Analysis Summary CMS-PAS-JME-10-003, CERN, 2010.

[33] M. Cacciari and G. P. Salam, "Pileup subtraction using jet areas", *Phys. Lett. B* **659** (2008) 119, doi:10.1016/j.physletb.2007.09.077, arXiv:0707.1378.

[34] CMS Collaboration, "Determination of jet energy calibration and transverse momentum resolution in CMS", *JINST* **6** (2011) P11002, doi:10.1088/1748-0221/6/11/P11002, arXiv:1107.4277.

[35] CMS Collaboration, "Identification of b quark jets at the CMS experiment in the LHC Run 2", CMS Physics Analysis Summary CMS-PAS-BTV-15-001, CERN, 2016.

[36] UA1 Collaboration, "Experimental Observation of Isolated Large Transverse Energy Electrons with Associated Missing Energy at $\sqrt{s} = 540$ GeV", *Phys. Lett. B* **122** (1983) 103, doi:10.1016/0370-2693(83)91177-2.

[37] J. Alwall et al., "The automated computation of tree-level and next-to-leading order differential cross sections, and their matching to parton shower simulations", *JHEP* **07** (2014) 079, doi:10.1007/JHEP07(2014)079, arXiv:1405.0301.

[38] P. Nason, "A new method for combining NLO QCD with shower Monte Carlo algorithms", *JHEP* **11** (2004) 040, doi:10.1088/1126-6708/2004/11/040, arXiv:hep-ph/0409146.

[39] S. Frixione, P. Nason, and C. Oleari, "Matching NLO QCD computations with Parton Shower simulations: the POWHEG method", *JHEP* **11** (2007) 070, doi:10.1088/1126-6708/2007/11/070, arXiv:0709.2092.

[40] S. Alioli, P. Nason, C. Oleari, and E. Re, "A general framework for implementing NLO calculations in shower Monte Carlo programs: the POWHEG BOX", *JHEP* **06** (2010) 043, doi:10.1007/JHEP06(2010)043, arXiv:1002.2581.

[41] S. Alioli, P. Nason, C. Oleari, and E. Re, "NLO single-top production matched with shower in POWHEG: s- and t-channel contributions", *JHEP* **09** (2009) 111, doi:10.1088/1126-6708/2009/09/111, arXiv:0907.4076. [Erratum: doi:10.1007/JHEP02(2010)011].

[42] E. Re, "Single-top Wt-channel production matched with parton showers using the POWHEG method", *Eur. Phys. J. C* **71** (2011) 1547, doi:10.1140/epjc/s10052-011-1547-z, arXiv:1009.2450.

[43] GEANT4 Collaboration, "GEANT4—a simulation toolkit", *Nucl. Instrum. Meth. A* **506** (2003) 250, doi:10.1016/S0168-9002(03)01368-8.

[44] T. Melia, P. Nason, R. Rontsch, and G. Zanderighi, "W^+W^-, WZ and ZZ production in the POWHEG BOX", *JHEP* **11** (2011) 078, doi:10.1007/JHEP11(2011)078, arXiv:1107.5051.

[45] M. Beneke, P. Falgari, S. Klein, and C. Schwinn, "Hadronic top-quark pair production with NNLL threshold resummation", *Nucl. Phys. B* **855** (2012) 695, doi:10.1016/j.nuclphysb.2011.10.021, arXiv:1109.1536.

[46] M. Cacciari et al., "Top-pair production at hadron colliders with next-to-next-to-leading logarithmic soft-gluon resummation", *Phys. Lett. B* **710** (2012) 612, doi:10.1016/j.physletb.2012.03.013, arXiv:1111.5869.

[47] P. Bärnreuther, M. Czakon, and A. Mitov, "Percent Level Precision Physics at the Tevatron: First Genuine NNLO QCD Corrections to $q\bar{q} \to t\bar{t} + X$", *Phys. Rev. Lett.* **109** (2012) 132001, doi:10.1103/PhysRevLett.109.132001, arXiv:1204.5201.

[48] M. Czakon and A. Mitov, "NNLO corrections to top-pair production at hadron colliders: the all-fermionic scattering channels", *JHEP* **12** (2012) 054, doi:10.1007/JHEP12(2012)054, arXiv:1207.0236.

[49] M. Czakon and A. Mitov, "NNLO corrections to top pair production at hadron colliders: the quark-gluon reaction", *JHEP* **01** (2013) 080, doi:10.1007/JHEP01(2013)080, arXiv:1210.6832.

[50] M. Czakon, P. Fiedler, and A. Mitov, "Total Top-Quark Pair-Production Cross Section at Hadron Colliders Through $O(\alpha_S^4)$", *Phys. Rev. Lett.* **110** (2013) 252004, doi:10.1103/PhysRevLett.110.252004, arXiv:1303.6254.

[51] R. Gavin, Y. Li, F. Petriello, and S. Quackenbush, "W Physics at the LHC with FEWZ 2.1", *Comput. Phys. Commun.* **184** (2013) 208, doi:10.1016/j.cpc.2012.09.005, arXiv:1201.5896.

[52] R. Gavin, Y. Li, F. Petriello, and S. Quackenbush, "FEWZ 2.0: A code for hadronic Z production at next-to-next-to-leading order", *Comput. Phys. Commun.* **182** (2011) 2388, doi:10.1016/j.cpc.2011.06.008, arXiv:1011.3540.

[53] T. Sjöstrand et al., "An Introduction to PYTHIA 8.2", *Comput. Phys. Commun.* **191** (2015) 159, doi:10.1016/j.cpc.2015.01.024, arXiv:1410.3012.

[54] W. Beenakker, R. Höpker, M. Spira, and P. M. Zerwas, "Squark and gluino production at hadron colliders", *Nucl. Phys. B* **492** (1997) 51, doi:10.1016/S0550-3213(97)00084-9, arXiv:hep-ph/9610490.

[55] A. Kulesza and L. Motyka, "Threshold resummation for squark-antisquark and gluino-pair production at the LHC", *Phys. Rev. Lett.* **102** (2009) 111802, doi:10.1103/PhysRevLett.102.111802, arXiv:0807.2405.

[56] A. Kulesza and L. Motyka, "Soft gluon resummation for the production of gluino-gluino and squark-antisquark pairs at the LHC", *Phys. Rev. D* **80** (2009) 095004, doi:10.1103/PhysRevD.80.095004, arXiv:0905.4749.

[57] W. Beenakker et al., "Soft-gluon resummation for squark and gluino hadroproduction", *JHEP* **12** (2009) 041, doi:10.1088/1126-6708/2009/12/041, arXiv:0909.4418.

[58] W. Beenakker et al., "Squark and gluino hadroproduction", *Int. J. Mod. Phys. A* **26** (2011) 2637, doi:10.1142/S0217751X11053560, arXiv:1105.1110.

[59] CMS Collaboration, "Fast simulation of the CMS detector", *J. Phys. Conf. Ser.* **219** (2010) 032053, doi:10.1088/1742-6596/219/3/032053.

[60] CMS Collaboration, "Comparison of the fast simulation of CMS with the first LHC data", CMS Detector Performance Summary CMS-DP-2010-039, CERN, 2010.

[61] NNPDF Collaboration, "Parton distributions for the LHC Run II", *JHEP* **04** (2015) 040, doi:10.1007/JHEP04(2015)040, arXiv:1410.8849.

[62] S. Catani, D. de Florian, M. Grazzini, and P. Nason, "Soft gluon resummation for Higgs boson production at hadron colliders", *JHEP* **07** (2003) 028, doi:10.1088/1126-6708/2003/07/028, arXiv:hep-ph/0306211.

[63] M. Cacciari et al., "The $t\bar{t}$ cross-section at 1.8 TeV and 1.96 TeV: a study of the systematics due to parton densities and scale dependence", *JHEP* **04** (2004) 068, doi:10.1088/1126-6708/2004/04/068, arXiv:hep-ph/0303085.

[64] CMS Collaboration, "Search for top-squark pair production in the single-lepton final state in pp collisions at $\sqrt{s}$ = 8 TeV", *Eur. Phys. J. C* **73** (2013) 2677, doi:10.1140/epjc/s10052-013-2677-2, arXiv:1308.1586.

[65] CMS Collaboration, "Search for new physics with jets and missing transverse momentum in pp collisions at $\sqrt{s} = 7$ TeV", *JHEP* **08** (2011) 155, doi:10.1007/JHEP08(2011)155, arXiv:1106.4503.

[66] CMS Collaboration, "Search for new physics in the multijet and missing transverse momentum final state in proton-proton collisions at $\sqrt{s} = 7$ TeV", *Phys. Rev. Lett.* **109** (2012) 171803, doi:10.1103/PhysRevLett.109.171803, arXiv:1207.1898.

[67] Particle Data Group, K. A. Olive et al., "Review of particle physics", *Chin. Phys. C* **38** (2014) 090001, doi:10.1088/1674-1137/38/9/090001.

[68] CMS Collaboration, " Observation of top quark pairs produced in association with a vector boson in pp collisions at $\sqrt{s} = 8$ TeV", *JHEP* **01** (2016) 096, doi:10.1007/JHEP01(2016)096, arXiv:1510.01131.

[69] CMS Collaboration, "Search for supersymmetry in events with b-quark jets and missing transverse energy in pp collisions at 7 TeV", *Phys. Rev. D* **86** (2012) 072010, doi:10.1103/PhysRevD.86.072010, arXiv:1208.4859.

[70] G. Cowan, K. Cranmer, E. Gross, and O. Vitells, "Asymptotic formulae for likelihood-based tests of new physics", *Eur. Phys. J. C* **71** (2011) 1554, doi:10.1140/epjc/s10052-011-1554-0, arXiv:1007.1727. [Erratum: doi:10.1140/epjc/s10052-013-2501-z].

[71] T. Junk, "Confidence level computation for combining searches with small statistics", *Nucl. Instr. and Meth. A* **434** (1999) 435, doi:10.1016/S0168-9002(99)00498-2, arXiv:hep-ex/9902006.

[72] A. L. Read, "Presentation of search results: the CL_s technique", *J. Phys. G* **28** (2002) 2693, doi:10.1088/0954-3899/28/10/313.

[73] ATLAS and CMS Collaborations, "Procedure for the LHC Higgs boson search combination in Summer 2011", Technical Report CMS-NOTE-2011-005, ATL-PHYS-PUB-2011-11, 2011.

[74] C. Borschensky et al., "Squark and gluino production cross sections in pp collisions at $\sqrt{s}$ = 13, 14, 33 and 100 TeV", *Eur. Phys. J. C* **74** (2014) 3174, doi:10.1140/epjc/s10052-014-3174-y, arXiv:1407.5066.

A Selection efficiency for example signal models

Table A.1: Absolute cumulative efficiencies in % for each step of the event selection process, listed for three representative signal models and choices for the gluino and LSP masses. Only statistical uncertainties are shown.

Selection		$pp \to \tilde{g}\tilde{g}, \tilde{g} \to b\bar{b}\tilde{\chi}_1^0$ $m_{\tilde{g}} = 1500\,\text{GeV}$ $m_{\tilde{\chi}_1^0} = 100\,\text{GeV}$	$pp \to \tilde{g}\tilde{g}, \tilde{g} \to t\bar{t}\tilde{\chi}_1^0$ $m_{\tilde{g}} = 1500\,\text{GeV}$ $m_{\tilde{\chi}_1^0} = 100\,\text{GeV}$	$pp \to \tilde{g}\tilde{g}, \tilde{g} \to q\bar{q}\tilde{\chi}_1^0$ $m_{\tilde{g}} = 1000\,\text{GeV}$ $m_{\tilde{\chi}_1^0} = 800\,\text{GeV}$
N_{jet}	≥ 4	96.49 ± 0.08	99.96 ± 0.01	76.87 ± 0.14
H_{T}	$> 500\,\text{GeV}$	96.46 ± 0.08	99.89 ± 0.01	38.30 ± 0.16
$H_{\text{T}}^{\text{miss}}$	$> 200\,\text{GeV}$	87.21 ± 0.15	88.65 ± 0.10	24.46 ± 0.14
N_{muon}	$= 0$	86.59 ± 0.15	56.00 ± 0.15	24.42 ± 0.14
N_{electron}	$= 0$	85.95 ± 0.15	35.21 ± 0.15	24.26 ± 0.14
$N_{\text{isolated tracks}}^{(\text{muon})}$	$= 0$	85.66 ± 0.15	34.46 ± 0.15	24.19 ± 0.14
$N_{\text{isolated tracks}}^{(\text{electron})}$	$= 0$	85.17 ± 0.16	33.50 ± 0.15	24.00 ± 0.14
$N_{\text{isolated tracks}}^{(\text{hadron})}$	$= 0$	84.20 ± 0.16	31.57 ± 0.14	23.26 ± 0.14
$\Delta\phi_{H_{\text{T}}^{\text{miss}}, j_i}$	$> 0.5, 0.5, 0.3, 0.3$	62.00 ± 0.21	23.96 ± 0.13	17.66 ± 0.12

B Prefit background predictions

Table B.1: Observed numbers of events and prefit background predictions for $4 \leq N_{\text{jet}} \leq 6$. These results are displayed in the leftmost section of Fig. 6. The first uncertainty is statistical and the second systematic.

Bin	$H_{\text{T}}^{\text{miss}}$ [GeV]	H_{T} [GeV]	$N_{\text{b-jet}}$	Lost-e/μ	$\tau \to$ had	$\text{Z} \to \nu\bar{\nu}$	QCD	Total Pred.	Obs.
1	200-500	500-800	0	$319 \pm 12 \pm 29$	$310 \pm 11 \pm 19$	$630 \pm 13^{+100}_{-80}$	$220 \pm 4 \pm 110$	$1480 \pm 26^{+150}_{-140}$	1602
2	200-500	800-1200	0	$59.2 \pm 4.3 \pm 5.4$	$69.1 \pm 5.2 \pm 5.7$	$145 \pm 6^{+26}_{-20}$	$100 \pm 2 \pm 34$	$373 \pm 12 \pm 42$	390
3	200-500	1200+	0	$13.8 \pm 2.2 \pm 1.4$	$14.4 \pm 2.5 \pm 1.6$	$31 \pm 3^{+12}_{-8}$	$90 \pm 2 \pm 24$	$150 \pm 6 \pm 27$	149
4	500-750	500-1200	0	$11.5 \pm 1.8 \pm 1.6$	$8.9 \pm 1.7 \pm 1.3$	$62 \pm 4^{+18}_{-13}$	$0.38^{+0.12+0.42}_{-0.09-0.29}$	$82 \pm 6^{+19}_{-13}$	120
5	500-750	1200+	0	$2.0 \pm 1.0 \pm 0.5$	$0.56^{+0.52}_{-0.25} \pm 0.15$	$5.5 \pm 1.3^{+2.1}_{-1.5}$	$1.0 \pm 0.2 \pm 0.9$	$8.9^{+2.1+2.4}_{-1.8-1.8}$	13
6	750+	800+	0	$1.39^{+0.93}_{-0.77} \pm 0.24$	$1.77^{+0.99}_{-0.88} \pm 0.34$	$10.4 \pm 1.8^{+5.8}_{-4.1}$	$0.24^{+0.09+0.26}_{-0.06-0.18}$	$13.8 \pm 2.6^{+5.8}_{-4.1}$	12
7	200-500	500-800	1	$171 \pm 8 \pm 17$	$206 \pm 9 \pm 13$	$127 \pm 21 \pm 29$	$69 \pm 2 \pm 37$	$574 \pm 27 \pm 52$	499
8	200-500	800-1200	1	$31.4 \pm 4.0 \pm 3.0$	$30.4 \pm 3.2 \pm 2.0$	$29.2 \pm 4.9^{+7.4}_{-6.7}$	$36 \pm 1 \pm 14$	$127 \pm 9 \pm 16$	123
9	200-500	1200+	1	$6.3 \pm 1.7 \pm 0.8$	$8.9 \pm 2.0 \pm 0.9$	$6.3 \pm 1.2^{+2.7}_{-2.0}$	$32 \pm 1 \pm 11$	$54 \pm 4 \pm 11$	44
10	500-750	500-1200	1	$3.1 \pm 1.1 \pm 0.6$	$2.64^{+0.96}_{-0.85} \pm 0.48$	$12.4 \pm 2.2^{+4.3}_{-3.5}$	$0.07^{+0.04+0.09}_{-0.02-0.05}$	$18.2 \pm 3.0^{+4.4}_{-3.6}$	22
11	500-750	1200+	1	$0.00^{+0.52}_{-0.00} \pm 0.00$	$0.07^{+0.46}_{-0.04} \pm 0.02$	$1.10 \pm 0.32^{+0.47}_{-0.36}$	$0.38^{+0.12+0.41}_{-0.09-0.29}$	$1.6^{+1.0}_{-0.3} \pm 0.5$	1
12	750+	800+	1	$0.00^{+0.50}_{-0.00} \pm 0.00$	$0.54^{+0.56}_{-0.32} \pm 0.13$	$2.1 \pm 0.5^{+1.2}_{-0.9}$	$0.02^{+0.06+0.06}_{-0.00-0.02}$	$2.6^{+1.2+1.2}_{-0.6-0.9}$	2
13	200-500	500-800	2	$71.9 \pm 6.1^{+7.2}_{-6.7}$	$77.2 \pm 5.0 \pm 5.4$	$28 \pm 8 \pm 12$	$15.9 \pm 1.1 \pm 8.8$	$193 \pm 14 \pm 17$	202
14	200-500	800-1200	2	$18.8 \pm 4.8^{+2.5}_{-2.2}$	$17.3 \pm 2.7 \pm 1.3$	$6.4 \pm 1.9 \pm 2.9$	$9.5 \pm 0.6 \pm 3.8$	$52.0 \pm 7.7 \pm 5.4$	45
15	200-500	1200+	2	$2.1 \pm 1.1 \pm 0.2$	$3.3 \pm 1.3 \pm 0.3$	$1.39 \pm 0.42 \pm 0.73$	$5.6 \pm 0.5 \pm 2.0$	$12.3 \pm 2.5 \pm 2.2$	15
16	500-750	500-1200	2	$1.9 \pm 1.7^{+0.7}_{-0.2}$	$2.26 \pm 0.88 \pm 0.86$	$2.7 \pm 0.8 \pm 1.4$	$0.03^{+0.02+0.04}_{-0.01-0.02}$	$6.9 \pm 2.8 \pm 1.6$	5
17	500-750	1200+	2	$3.3 \pm 3.4^{+1.4}_{-0.0}$	$0.07^{+0.46+0.02}_{-0.05-0.01}$	$0.24 \pm 0.09 \pm 0.13$	$0.07^{+0.08+0.09}_{-0.04-0.03}$	$3.7^{+3.8+0.2}_{-3.4-0.1}$	0
18	750+	800+	2	$0.00^{+0.46}_{-0.00} \pm 0.00$	$0.04^{+0.46+0.02}_{-0.03-0.01}$	$0.46 \pm 0.15^{+0.32}_{-0.26}$	$0.03^{+0.06+0.05}_{-0.02-0.01}$	$0.53^{+0.93+0.32}_{-0.16-0.26}$	1
19	200-500	500-800	3+	$6.3 \pm 1.7 \pm 0.8$	$10.8 \pm 2.2 \pm 1.6$	$6.5 \pm 3.8 \pm 2.9$	$1.21^{+0.37}_{-0.29} \pm 0.82$	$24.8 \pm 5.4 \pm 3.5$	17
20	200-500	800-1200	3+	$0.24^{+0.67+0.03}_{-0.24-0.00}$	$1.10^{+0.61}_{-0.40} \pm 0.15$	$1.49 \pm 0.87^{+0.70}_{-0.62}$	$0.70^{+0.20}_{-0.16} \pm 0.37$	$3.5^{+1.6}_{-1.1} \pm 0.8$	7
21	200-500	1200+	3+	$0.80^{+0.91}_{-0.57} \pm 0.13$	$0.11^{+0.46}_{-0.05} \pm 0.02$	$0.32 \pm 0.19^{+0.19}_{-0.13}$	$0.72^{+0.23}_{-0.18} \pm 0.36$	$2.0^{+1.4}_{-0.7} \pm 0.4$	3
22	500-750	500-1200	3+	$0.00^{+0.63}_{-0.00} \pm 0.00$	$0.03^{+0.46}_{-0.01} \pm 0.01$	$0.63 \pm 0.37^{+0.33}_{-0.26}$	$0.05^{+0.11+0.09}_{-0.04-0.01}$	$0.7^{+1.2}_{-0.4} \pm 0.3$	0
23	500-750	1200+	3+	$0.00^{+0.77}_{-0.00} \pm 0.00$	$0.00^{+0.46}_{-0.00} \pm 0.00$	$0.06 \pm 0.04^{+0.03}_{-0.02}$	$0.00^{+0.05+0.02}_{-0.00-0.00}$	$0.1^{+1.2+0.1}_{-0.1-0.0}$	0
24	750+	800+	3+	$0.00^{+0.58}_{-0.00} \pm 0.00$	$0.00^{+0.46}_{-0.00} \pm 0.00$	$0.11 \pm 0.06^{+0.08}_{-0.04}$	$0.00^{+0.04+0.02}_{-0.00-0.00}$	$0.1^{+1.0+0.1}_{-0.1-0.0}$	0

Table B.2: Observed numbers of events and prefit background predictions for $7 \leq N_{\text{jet}} \leq 8$. These results are displayed in the central section of Fig. 6. The first uncertainty is statistical and the second systematic.

Bin	$H_{\text{T}}^{\text{miss}}$ [GeV]	H_{T} [GeV]	$N_{\text{b-jet}}$	Lost-e/μ	$\tau \to$ had	$\text{Z} \to \nu\bar{\nu}$	QCD	Total Pred.	Obs.
25	200-500	500-800	0	$18.8 \pm 3.1 \pm 2.3$	$24.5 \pm 2.7 \pm 2.0$	$27.4 \pm 2.8^{+6.7}_{-5.1}$	$14.1 \pm 1.6 \pm 8.2$	$85 \pm 7 \pm 11$	85
26	200-500	800-1200	0	$12.5 \pm 1.8 \pm 2.2$	$15.6 \pm 2.3 \pm 1.3$	$17.3 \pm 2.3^{+4.2}_{-3.2}$	$16.3 \pm 1.2 \pm 7.1$	$61.7 \pm 4.8 \pm 8.4$	60
27	200-500	1200+	0	$2.9 \pm 1.2 \pm 0.3$	$3.5 \pm 1.3 \pm 0.3$	$6.0 \pm 1.3^{+2.3}_{-1.7}$	$23.0 \pm 1.6 \pm 8.8$	$35.4 \pm 3.1 \pm 9.0$	42
28	500-750	500-1200	0	$0.53^{+0.45}_{-0.26} \pm 0.13$	$0.81^{+0.66}_{-0.47} \pm 0.19$	$0.36 \pm 0.36^{+0.12}_{-0.00}$	$0.06^{+0.10+0.09}_{-0.04-0.02}$	$1.8^{+1.2}_{-0.8} \pm 0.3$	1
29	500-750	1200+	0	$1.03^{+0.88+0.33}_{-0.80-0.24}$	$1.44^{+0.93}_{-0.80} \pm 0.29$	$0.60 \pm 0.43^{+0.26}_{-0.18}$	$0.26^{+0.17+0.30}_{-0.11-0.15}$	$3.3 \pm 1.8 \pm 0.5$	1
30	750+	800+	0	$0.17^{+0.38+0.09}_{-0.17-0.00}$	$0.17^{+0.49+0.11}_{-0.17-0.00}$	$0.56 \pm 0.40^{+0.34}_{-0.16}$	$0.19^{+0.16+0.23}_{-0.09-0.10}$	$1.09^{+0.97+0.41}_{-0.53-0.19}$	1
31	200-500	500-800	1	$25.8 \pm 2.9 \pm 3.1$	$31.8 \pm 3.0 \pm 2.3$	$11.7 \pm 2.2 \pm 3.7$	$8.1 \pm 1.3 \pm 5.1$	$77.3 \pm 6.4 \pm 7.3$	63
32	200-500	800-1200	1	$9.0 \pm 1.6 \pm 1.2$	$14.4 \pm 2.0 \pm 1.4$	$7.4 \pm 1.5 \pm 2.3$	$7.6 \pm 0.8 \pm 3.7$	$38.3 \pm 4.0 \pm 4.7$	43
33	200-500	1200+	1	$3.3 \pm 1.1 \pm 0.4$	$6.3 \pm 1.5 \pm 0.7$	$2.6 \pm 0.7 \pm 1.1$	$13.7 \pm 1.2 \pm 5.9$	$25.9 \pm 2.9 \pm 6.1$	29
34	500-750	500-1200	1	$0.46^{+0.49}_{-0.27} \pm 0.11$	$0.51^{+0.55}_{-0.29} \pm 0.11$	$0.15 \pm 0.16^{+0.06}_{-0.00}$	$0.00^{+0.12+0.05}_{-0.00-0.00}$	$1.1^{+1.1}_{-0.6} \pm 0.2$	2
35	500-750	1200+	1	$0.00^{+0.40}_{-0.00} \pm 0.00$	$0.25^{+0.49}_{-0.18} \pm 0.05$	$0.26 \pm 0.19^{+0.12}_{-0.07}$	$0.12^{+0.14+0.16}_{-0.07-0.05}$	$0.63^{+0.92+0.21}_{-0.27-0.10}$	2
36	750+	800+	1	$0.00^{+0.45}_{-0.00} \pm 0.00$	$0.02^{+0.46+0.01}_{-0.01-0.00}$	$0.24 \pm 0.17^{+0.15}_{-0.07}$	$0.00^{+0.08+0.03}_{-0.00-0.00}$	$0.25^{+0.93+0.16}_{-0.17-0.07}$	1
37	200-500	500-800	2	$13.2 \pm 2.2 \pm 1.5$	$16.0 \pm 1.9 \pm 1.2$	$4.8 \pm 1.5 \pm 2.4$	$0.16^{+0.32+0.57}_{-0.00-0.16}$	$34.1 \pm 4.3 \pm 3.1$	32
38	200-500	800-1200	2	$6.3 \pm 1.3 \pm 0.7$	$10.7 \pm 1.8 \pm 0.9$	$3.0 \pm 1.0 \pm 1.5$	$2.2 \pm .5 \pm 1.1$	$22.2 \pm 3.3 \pm 2.2$	17
39	200-500	1200+	2	$1.73^{+0.79}_{-0.62} \pm 0.20$	$1.89^{+0.88}_{-0.75} \pm 0.18$	$1.06 \pm 0.38 \pm 0.60$	$3.6 \pm 0.6 \pm 1.6$	$8.2 \pm 1.7 \pm 1.8$	4
40	500-750	500-1200	2	$0.00^{+0.39}_{-0.00} \pm 0.00$	$0.04^{+0.46}_{-0.02} \pm 0.01$	$0.06^{+0.07+0.03}_{-0.06-0.00}$	$0.00^{+0.12+0.05}_{-0.00-0.00}$	$0.10^{+0.86+0.06}_{-0.06-0.01}$	0
41	500-750	1200+	2	$0.00^{+0.43}_{-0.00} \pm 0.00$	$0.07^{+0.47+0.04}_{-0.07-0.00}$	$0.11 \pm 0.08^{+0.06}_{-0.02}$	$0.03^{+0.11+0.05}_{-0.02-0.01}$	$0.21^{+0.90+0.08}_{-0.11-0.03}$	1
42	750+	800+	2	$0.00^{+0.34}_{-0.00} \pm 0.00$	$0.13^{+0.48+0.06}_{-0.13-0.00}$	$0.10 \pm 0.07^{+0.07}_{-0.02}$	$0.00^{+0.08+0.03}_{-0.00-0.00}$	$0.23^{+0.82+0.08}_{-0.15-0.02}$	0
43	200-500	500-800	3+	$3.9 \pm 1.2 \pm 0.5$	$5.8 \pm 1.3 \pm 0.7$	$2.5 \pm 1.5^{+1.8}_{-1.0}$	$1.09^{+0.62+0.86}_{-0.41-0.68}$	$13.3 \pm 3.0^{+2.1}_{-1.5}$	3
44	200-500	800-1200	3+	$0.44^{+0.49}_{-0.25} \pm 0.05$	$1.66^{+0.76}_{-0.60} \pm 0.26$	$1.6 \pm 1.0^{+1.1}_{-0.7}$	$0.60^{+0.30}_{-0.21} \pm 0.39$	$4.3^{+1.6+1.2}_{-1.3-0.8}$	4
45	200-500	1200+	3+	$0.66^{+0.72}_{-0.52} \pm 0.12$	$0.65^{+0.61}_{-0.40} \pm 0.10$	$0.56 \pm 0.35^{+0.42}_{-0.21}$	$0.04^{+0.19+0.12}_{-0.00-0.04}$	$1.9^{+1.4+0.5}_{-1.0-0.3}$	1
46	500-750	500-1200	3+	$0.00^{+0.52}_{-0.00} \pm 0.00$	$0.00^{+0.46}_{-0.00} \pm 0.00$	$0.03^{+0.04+0.02}_{-0.03-0.00}$	$0.04^{+0.09+0.07}_{-0.03-0.01}$	$0.07^{+0.98+0.07}_{-0.05-0.01}$	0
47	500-750	1200+	3+	$0.00^{+0.47}_{-0.00} \pm 0.00$	$0.00^{+0.46}_{-0.00} \pm 0.00$	$0.06 \pm 0.05^{+0.04}_{-0.00}$	$0.00^{+0.09+0.03}_{-0.00-0.00}$	$0.06^{+0.94+0.05}_{-0.05-0.00}$	0
48	750+	800+	3+	$0.00^{+0.61}_{-0.00} \pm 0.00$	$0.01^{+0.46+0.01}_{-0.01-0.00}$	$0.05 \pm 0.05^{+0.05}_{-0.00}$	$0.00^{+0.08+0.03}_{-0.00-0.00}$	$0.1^{+1.1+0.1}_{-0.1-0.0}$	0

Table B.3: Observed numbers of events and prefit background predictions for $N_{\text{jet}} \geq 9$. These results are displayed in the rightmost section of Fig. 6. The first uncertainty is statistical and the second systematic.

Bin	$H_{\text{T}}^{\text{miss}}$ [GeV]	H_{T} [GeV]	$N_{\text{b-jet}}$	Lost-e/μ	$\tau \to$ had	$\text{Z} \to \nu\bar{\nu}$	QCD	Total Pred.	Obs.
49	200-500	500-800	0	$0.99^{+0.59}_{-0.45} \pm 0.21$	$0.61^{+0.52}_{-0.23} \pm 0.09$	$0.26 \pm 0.26^{+0.12}_{-0.00}$	$0.92^{+0.54+0.80}_{-0.35-0.57}$	$2.8^{+1.3}_{-0.8} \pm 0.7$	2
50	200-500	800-1200	0	$2.12^{+0.72}_{-0.62} \pm 0.33$	$3.9 \pm 1.2 \pm 0.4$	$2.14 \pm 0.81^{+0.81}_{-0.64}$	$0.78^{+0.31}_{-0.23} \pm 0.55$	$9.0 \pm 2.0 \pm 1.1$	12
51	200-500	1200+	0	$0.58^{+0.54}_{-0.35} \pm 0.08$	$1.05^{+0.76}_{-0.61} \pm 0.15$	$0.42 \pm 0.30^{+0.18}_{-0.12}$	$3.9 \pm 0.7 \pm 2.5$	$6.0^{+1.5}_{-1.2} \pm 2.5$	8
52	500-750	500-1200	0	$0.00^{+0.34}_{-0.00} \pm 0.00$	$0.00^{+0.46}_{-0.00} \pm 0.00$	$0.15 \pm 0.15^{+0.11}_{-0.00}$	$0.00^{+0.11+0.04}_{-0.00-0.00}$	$0.15^{+0.82+0.11}_{-0.15-0.00}$	0
53	500-750	1200+	0	$0.14^{+0.36+0.05}_{-0.14-0.00}$	$0.02^{+0.46+0.01}_{-0.02-0.00}$	$0.00^{+0.76}_{-0.00} \pm 0.00$	$0.00^{+0.09+0.04}_{-0.00-0.00}$	$0.2^{+1.1+0.1}_{-0.2-0.0}$	0
54	750+	800+	0	$0.00^{+0.28}_{-0.00} \pm 0.00$	$0.00^{+0.46}_{-0.00} \pm 0.00$	$0.00^{+0.79}_{-0.00} \pm 0.00$	$0.00^{+0.08+0.03}_{-0.00-0.00}$	$0.0^{+1.1+0.1}_{-0.0-0.0}$	0
55	200-500	500-800	1	$1.36^{+0.66}_{-0.53} \pm 0.19$	$1.58^{+0.71}_{-0.54} \pm 0.19$	$0.19 \pm 0.19^{+0.10}_{-0.00}$	$0.09^{+0.22+0.15}_{-0.07-0.02}$	$3.2^{+1.4}_{-1.1} \pm 0.3$	6
56	200-500	800-1200	1	$3.19^{+0.99}_{-0.91} \pm 0.52$	$4.1 \pm 1.2 \pm 0.4$	$1.57 \pm 0.64 \pm 0.68$	$0.88^{+0.34}_{-0.25} \pm 0.64$	$9.7 \pm 2.2 \pm 1.2$	4
57	200-500	1200+	1	$1.70^{+0.85}_{-0.73} \pm 0.25$	$1.41^{+0.79}_{-0.65} \pm 0.25$	$0.31 \pm 0.22^{+0.15}_{-0.08}$	$2.4 \pm 0.5 \pm 1.6$	$5.8 \pm 1.6 \pm 1.7$	3
58	500-750	500-1200	1	$0.00^{+0.40}_{-0.00} \pm 0.00$	$0.05^{+0.46+0.02}_{-0.05-0.00}$	$0.11 \pm 0.11^{+0.08}_{-0.00}$	$0.00^{+0.11+0.04}_{-0.00-0.00}$	$0.16^{+0.88+0.09}_{-0.12-0.00}$	0
59	500-750	1200+	1	$0.00^{+0.41}_{-0.00} \pm 0.00$	$0.15^{+0.48+0.04}_{-0.14-0.00}$	$0.00^{+0.66}_{-0.00} \pm 0.00$	$0.00^{+0.09+0.03}_{-0.00-0.00}$	$0.2^{+1.1+0.1}_{-0.1-0.0}$	1
60	750+	800+	1	$0.00^{+0.33}_{-0.00} \pm 0.00$	$0.00^{+0.46}_{-0.00} \pm 0.00$	$0.00^{+0.68}_{-0.00} \pm 0.00$	$0.00^{+0.08+0.03}_{-0.00-0.00}$	$0.0^{+1.1+0.1}_{-0.0-0.0}$	0
61	200-500	500-800	2	$1.38^{+0.74}_{-0.62} \pm 0.18$	$1.51^{+0.77}_{-0.61} \pm 0.15$	$0.10 \pm 0.10^{+0.07}_{-0.00}$	$0.00^{+0.22+0.11}_{-0.00-0.00}$	$3.0^{+1.5}_{-1.2} \pm 0.3$	3
62	200-500	800-1200	2	$1.39^{+0.68}_{-0.57} \pm 0.20$	$2.20^{+0.92}_{-0.80} \pm 0.20$	$0.87 \pm 0.41^{+0.54}_{-0.46}$	$0.26^{+0.22+0.24}_{-0.13-0.13}$	$4.7^{+1.7}_{-1.4} \pm 0.6$	1
63	200-500	1200+	2	$0.28^{+0.48}_{-0.20} \pm 0.04$	$1.40^{+0.83}_{-0.70} \pm 0.19$	$0.17 \pm 0.13^{+0.11}_{-0.04}$	$1.38^{+0.45}_{-0.35} \pm 0.95$	$3.2^{+1.4}_{-1.0} \pm 1.0$	2
64	500-750	500-1200	2	$0.00^{+0.36}_{-0.00} \pm 0.00$	$0.00^{+0.46}_{-0.00} \pm 0.00$	$0.06 \pm 0.06^{+0.05}_{-0.00}$	$0.00^{+0.11+0.04}_{-0.00-0.00}$	$0.06^{+0.83+0.07}_{-0.06-0.00}$	0
65	500-750	1200+	2	$0.00^{+0.45}_{-0.00} \pm 0.00$	$0.01^{+0.46}_{-0.01} \pm 0.00$	$0.00^{+0.52}_{-0.00} \pm 0.00$	$0.00^{+0.09+0.03}_{-0.00-0.00}$	$0.0^{+1.1+0.1}_{-0.0-0.0}$	0
66	750+	800+	2	$0.00^{+0.43}_{-0.00} \pm 0.00$	$0.00^{+0.46}_{-0.00} \pm 0.00$	$0.00^{+0.52}_{-0.00} \pm 0.00$	$0.00^{+0.08+0.03}_{-0.00-0.00}$	$0.0^{+1.0+0.1}_{-0.0-0.0}$	0
67	200-500	500-800	3+	$0.30^{+0.48}_{-0.21} \pm 0.05$	$1.13^{+0.79}_{-0.64} \pm 0.16$	$0.02^{+0.03+0.03}_{-0.02-0.00}$	$0.00^{+0.22+0.09}_{-0.00-0.00}$	$1.5^{+1.3}_{-0.9} \pm 0.2$	0
68	200-500	800-1200	3+	$1.9 \pm 1.4 \pm 0.3$	$0.70^{+0.60}_{-0.38} \pm 0.09$	$0.18 \pm 0.13^{+0.24}_{-0.06}$	$0.27^{+0.22+0.25}_{-0.13-0.14}$	$3.1^{+2.0}_{-1.7} \pm 0.5$	1
69	200-500	1200+	3+	$0.46^{+0.64+0.06}_{-0.46-0.00}$	$0.32^{+0.54}_{-0.28} \pm 0.04$	$0.04 \pm 0.03^{+0.05}_{-0.00}$	$0.04^{+0.10+0.07}_{-0.03-0.01}$	$0.9^{+1.2+0.1}_{-0.8-0.0}$	0
70	500-750	500-1200	3+	$0.13^{+0.47+0.05}_{-0.13-0.00}$	$0.00^{+0.46}_{-0.00} \pm 0.00$	$0.01^{+0.02+0.02}_{-0.01-0.00}$	$0.00^{+0.11+0.04}_{-0.00-0.00}$	$0.14^{+0.93+0.04}_{-0.13-0.00}$	0
71	500-750	1200+	3+	$0.00^{+0.41}_{-0.00} \pm 0.00$	$0.00^{+0.46}_{-0.00} \pm 0.00$	$0.00^{+0.30}_{-0.00} \pm 0.00$	$0.00^{+0.09+0.02}_{-0.00-0.00}$	$0.00^{+0.93+0.02}_{-0.00-0.00}$	0
72	750+	800+	3+	$0.00^{+0.44}_{-0.00} \pm 0.00$	$0.00^{+0.46}_{-0.00} \pm 0.00$	$0.00^{+0.28}_{-0.00} \pm 0.00$	$0.00^{+0.08+0.03}_{-0.00-0.00}$	$0.00^{+0.95+0.03}_{-0.00-0.00}$	0

C The CMS Collaboration

Yerevan Physics Institute, Yerevan, Armenia
V. Khachatryan, A.M. Sirunyan, A. Tumasyan

Institut für Hochenergiephysik der OeAW, Wien, Austria
W. Adam, E. Asilar, T. Bergauer, J. Brandstetter, E. Brondolin, M. Dragicevic, J. Erö, M. Flechl, M. Friedl, R. Frühwirth[1], V.M. Ghete, C. Hartl, N. Hörmann, J. Hrubec, M. Jeitler[1], A. König, I. Krätschmer, D. Liko, T. Matsushita, I. Mikulec, D. Rabady, N. Rad, B. Rahbaran, H. Rohringer, J. Schieck[1], J. Strauss, W. Treberer-Treberspurg, W. Waltenberger, C.-E. Wulz[1]

National Centre for Particle and High Energy Physics, Minsk, Belarus
V. Mossolov, N. Shumeiko, J. Suarez Gonzalez

Universiteit Antwerpen, Antwerpen, Belgium
S. Alderweireldt, T. Cornelis, E.A. De Wolf, X. Janssen, A. Knutsson, J. Lauwers, S. Luyckx, M. Van De Klundert, H. Van Haevermaet, P. Van Mechelen, N. Van Remortel, A. Van Spilbeeck

Vrije Universiteit Brussel, Brussel, Belgium
S. Abu Zeid, F. Blekman, J. D'Hondt, N. Daci, I. De Bruyn, K. Deroover, N. Heracleous, S. Lowette, S. Moortgat, L. Moreels, A. Olbrechts, Q. Python, S. Tavernier, W. Van Doninck, P. Van Mulders, I. Van Parijs

Université Libre de Bruxelles, Bruxelles, Belgium
H. Brun, C. Caillol, B. Clerbaux, G. De Lentdecker, H. Delannoy, G. Fasanella, L. Favart, R. Goldouzian, A. Grebenyuk, G. Karapostoli, T. Lenzi, A. Léonard, T. Maerschalk, A. Marinov, A. Randle-conde, T. Seva, C. Vander Velde, P. Vanlaer, R. Yonamine, F. Zenoni, F. Zhang[2]

Ghent University, Ghent, Belgium
A. Cimmino, D. Dobur, A. Fagot, G. Garcia, M. Gul, J. Mccartin, D. Poyraz, S. Salva, R. Schöfbeck, M. Tytgat, W. Van Driessche, E. Yazgan, N. Zaganidis

Université Catholique de Louvain, Louvain-la-Neuve, Belgium
C. Beluffi[3], O. Bondu, S. Brochet, G. Bruno, A. Caudron, L. Ceard, S. De Visscher, C. Delaere, M. Delcourt, L. Forthomme, B. Francois, A. Giammanco, A. Jafari, P. Jez, M. Komm, V. Lemaitre, A. Magitteri, A. Mertens, M. Musich, C. Nuttens, K. Piotrzkowski, L. Quertenmont, M. Selvaggi, M. Vidal Marono, S. Wertz

Université de Mons, Mons, Belgium
N. Beliy

Centro Brasileiro de Pesquisas Fisicas, Rio de Janeiro, Brazil
W.L. Aldá Júnior, F.L. Alves, G.A. Alves, L. Brito, M. Correa Martins Junior, C. Hensel, A. Moraes, M.E. Pol, P. Rebello Teles

Universidade do Estado do Rio de Janeiro, Rio de Janeiro, Brazil
E. Belchior Batista Das Chagas, W. Carvalho, J. Chinellato[4], A. Custódio, E.M. Da Costa, G.G. Da Silveira, D. De Jesus Damiao, C. De Oliveira Martins, S. Fonseca De Souza, L.M. Huertas Guativa, H. Malbouisson, D. Matos Figueiredo, C. Mora Herrera, L. Mundim, H. Nogima, W.L. Prado Da Silva, A. Santoro, A. Sznajder, E.J. Tonelli Manganote[4], A. Vilela Pereira

Universidade Estadual Paulista [a], Universidade Federal do ABC [b], São Paulo, Brazil
S. Ahuja[a], C.A. Bernardes[b], S. Dogra[a], T.R. Fernandez Perez Tomei[a], E.M. Gregores[b],

P.G. Mercadante[b], C.S. Moon[a,5], S.F. Novaes[a], Sandra S. Padula[a], D. Romero Abad[b], J.C. Ruiz Vargas

Institute for Nuclear Research and Nuclear Energy, Sofia, Bulgaria
A. Aleksandrov, R. Hadjiiska, P. Iaydjiev, M. Rodozov, S. Stoykova, G. Sultanov, M. Vutova

University of Sofia, Sofia, Bulgaria
A. Dimitrov, I. Glushkov, L. Litov, B. Pavlov, P. Petkov

Beihang University, Beijing, China
W. Fang[6]

Institute of High Energy Physics, Beijing, China
M. Ahmad, J.G. Bian, G.M. Chen, H.S. Chen, M. Chen, Y. Chen[7], T. Cheng, R. Du, C.H. Jiang, D. Leggat, Z. Liu, F. Romeo, S.M. Shaheen, A. Spiezia, J. Tao, C. Wang, Z. Wang, H. Zhang, J. Zhao

State Key Laboratory of Nuclear Physics and Technology, Peking University, Beijing, China
C. Asawatangtrakuldee, Y. Ban, Q. Li, S. Liu, Y. Mao, S.J. Qian, D. Wang, Z. Xu

Universidad de Los Andes, Bogota, Colombia
C. Avila, A. Cabrera, L.F. Chaparro Sierra, C. Florez, J.P. Gomez, J.D. Ruiz Alvarez, J.C. Sanabria

University of Split, Faculty of Electrical Engineering, Mechanical Engineering and Naval Architecture, Split, Croatia
N. Godinovic, D. Lelas, I. Puljak, P.M. Ribeiro Cipriano

University of Split, Faculty of Science, Split, Croatia
Z. Antunovic, M. Kovac

Institute Rudjer Boskovic, Zagreb, Croatia
V. Brigljevic, D. Ferencek, K. Kadija, J. Luetic, S. Micanovic, L. Sudic

University of Cyprus, Nicosia, Cyprus
A. Attikis, G. Mavromanolakis, J. Mousa, C. Nicolaou, F. Ptochos, P.A. Razis, H. Rykaczewski

Charles University, Prague, Czech Republic
M. Finger[8], M. Finger Jr.[8]

Universidad San Francisco de Quito, Quito, Ecuador
E. Carrera Jarrin

Academy of Scientific Research and Technology of the Arab Republic of Egypt, Egyptian Network of High Energy Physics, Cairo, Egypt
A.A. Abdelalim[9,10], E. El-khateeb[11,11], M.A. Mahmoud[12,13], A. Radi[13,11]

National Institute of Chemical Physics and Biophysics, Tallinn, Estonia
B. Calpas, M. Kadastik, M. Murumaa, L. Perrini, M. Raidal, A. Tiko, C. Veelken

Department of Physics, University of Helsinki, Helsinki, Finland
P. Eerola, J. Pekkanen, M. Voutilainen

Helsinki Institute of Physics, Helsinki, Finland
J. Härkönen, V. Karimäki, R. Kinnunen, T. Lampén, K. Lassila-Perini, S. Lehti, T. Lindén, P. Luukka, T. Peltola, J. Tuominiemi, E. Tuovinen, L. Wendland

Lappeenranta University of Technology, Lappeenranta, Finland
J. Talvitie, T. Tuuva

DSM/IRFU, CEA/Saclay, Gif-sur-Yvette, France
M. Besancon, F. Couderc, M. Dejardin, D. Denegri, B. Fabbro, J.L. Faure, C. Favaro, F. Ferri, S. Ganjour, S. Ghosh, A. Givernaud, P. Gras, G. Hamel de Monchenault, P. Jarry, E. Locci, M. Machet, J. Malcles, J. Rander, A. Rosowsky, M. Titov, A. Zghiche

Laboratoire Leprince-Ringuet, Ecole Polytechnique, IN2P3-CNRS, Palaiseau, France
A. Abdulsalam, I. Antropov, S. Baffioni, F. Beaudette, P. Busson, L. Cadamuro, E. Chapon, C. Charlot, O. Davignon, R. Granier de Cassagnac, M. Jo, S. Lisniak, P. Miné, I.N. Naranjo, M. Nguyen, C. Ochando, G. Ortona, P. Paganini, P. Pigard, S. Regnard, R. Salerno, Y. Sirois, T. Strebler, Y. Yilmaz, A. Zabi

Institut Pluridisciplinaire Hubert Curien, Université de Strasbourg, Université de Haute Alsace Mulhouse, CNRS/IN2P3, Strasbourg, France
J.-L. Agram[14], J. Andrea, A. Aubin, D. Bloch, J.-M. Brom, M. Buttignol, E.C. Chabert, N. Chanon, C. Collard, E. Conte[14], X. Coubez, J.-C. Fontaine[14], D. Gelé, U. Goerlach, A.-C. Le Bihan, J.A. Merlin[15], K. Skovpen, P. Van Hove

Centre de Calcul de l'Institut National de Physique Nucleaire et de Physique des Particules, CNRS/IN2P3, Villeurbanne, France
S. Gadrat

Université de Lyon, Université Claude Bernard Lyon 1, CNRS-IN2P3, Institut de Physique Nucléaire de Lyon, Villeurbanne, France
S. Beauceron, C. Bernet, G. Boudoul, E. Bouvier, C.A. Carrillo Montoya, R. Chierici, D. Contardo, B. Courbon, P. Depasse, H. El Mamouni, J. Fan, J. Fay, S. Gascon, M. Gouzevitch, G. Grenier, B. Ille, F. Lagarde, I.B. Laktineh, M. Lethuillier, L. Mirabito, A.L. Pequegnot, S. Perries, A. Popov[16], D. Sabes, V. Sordini, M. Vander Donckt, P. Verdier, S. Viret

Georgian Technical University, Tbilisi, Georgia
A. Khvedelidze[8]

Tbilisi State University, Tbilisi, Georgia
Z. Tsamalaidze[8]

RWTH Aachen University, I. Physikalisches Institut, Aachen, Germany
C. Autermann, S. Beranek, L. Feld, A. Heister, M.K. Kiesel, K. Klein, M. Lipinski, A. Ostapchuk, M. Preuten, F. Raupach, S. Schael, C. Schomakers, J.F. Schulte, J. Schulz, T. Verlage, H. Weber, V. Zhukov[16]

RWTH Aachen University, III. Physikalisches Institut A, Aachen, Germany
M. Ata, M. Brodski, E. Dietz-Laursonn, D. Duchardt, M. Endres, M. Erdmann, S. Erdweg, T. Esch, R. Fischer, A. Güth, T. Hebbeker, C. Heidemann, K. Hoepfner, S. Knutzen, M. Merschmeyer, A. Meyer, P. Millet, S. Mukherjee, M. Olschewski, K. Padeken, P. Papacz, T. Pook, M. Radziej, H. Reithler, M. Rieger, F. Scheuch, L. Sonnenschein, D. Teyssier, S. Thüer

RWTH Aachen University, III. Physikalisches Institut B, Aachen, Germany
V. Cherepanov, Y. Erdogan, G. Flügge, H. Geenen, M. Geisler, F. Hoehle, B. Kargoll, T. Kress, A. Künsken, J. Lingemann, A. Nehrkorn, A. Nowack, I.M. Nugent, C. Pistone, O. Pooth, A. Stahl[15]

Deutsches Elektronen-Synchrotron, Hamburg, Germany
M. Aldaya Martin, I. Asin, K. Beernaert, O. Behnke, U. Behrens, A.A. Bin Anuar, K. Borras[17], A. Campbell, P. Connor, C. Contreras-Campana, F. Costanza, C. Diez Pardos, G. Dolinska, G. Eckerlin, D. Eckstein, T. Eichhorn, E. Gallo[18], J. Garay Garcia, A. Geiser,

A. Gizhko, J.M. Grados Luyando, P. Gunnellini, A. Harb, J. Hauk, M. Hempel[19], H. Jung, A. Kalogeropoulos, O. Karacheban[19], M. Kasemann, J. Kieseler, C. Kleinwort, I. Korol, W. Lange, A. Lelek, J. Leonard, K. Lipka, A. Lobanov, W. Lohmann[19], R. Mankel, I.-A. Melzer-Pellmann, A.B. Meyer, G. Mittag, J. Mnich, A. Mussgiller, E. Ntomari, D. Pitzl, R. Placakyte, A. Raspereza, B. Roland, M.Ö. Sahin, P. Saxena, T. Schoerner-Sadenius, C. Seitz, S. Spannagel, N. Stefaniuk, K.D. Trippkewitz, G.P. Van Onsem, R. Walsh, C. Wissing

University of Hamburg, Hamburg, Germany
V. Blobel, M. Centis Vignali, A.R. Draeger, T. Dreyer, J. Erfle, E. Garutti, K. Goebel, D. Gonzalez, M. Görner, J. Haller, M. Hoffmann, R.S. Höing, A. Junkes, R. Klanner, R. Kogler, N. Kovalchuk, S. Kurz, T. Lapsien, T. Lenz, I. Marchesini, D. Marconi, M. Meyer, M. Niedziela, D. Nowatschin, J. Ott, F. Pantaleo[15], T. Peiffer, A. Perieanu, N. Pietsch, J. Poehlsen, C. Sander, C. Scharf, P. Schleper, E. Schlieckau, A. Schmidt, S. Schumann, J. Schwandt, H. Stadie, G. Steinbrück, F.M. Stober, M. Stöver, H. Tholen, D. Troendle, E. Usai, L. Vanelderen, A. Vanhoefer, B. Vormwald

Institut für Experimentelle Kernphysik, Karlsruhe, Germany
C. Barth, C. Baus, J. Berger, E. Butz, T. Chwalek, F. Colombo, W. De Boer, A. Dierlamm, S. Fink, R. Friese, M. Giffels, A. Gilbert, D. Haitz, F. Hartmann[15], S.M. Heindl, U. Husemann, I. Katkov[16], A. Kornmayer[15], P. Lobelle Pardo, B. Maier, H. Mildner, M.U. Mozer, T. Müller, Th. Müller, M. Plagge, G. Quast, K. Rabbertz, S. Röcker, F. Roscher, M. Schröder, G. Sieber, H.J. Simonis, R. Ulrich, J. Wagner-Kuhr, S. Wayand, M. Weber, T. Weiler, S. Williamson, C. Wöhrmann, R. Wolf

Institute of Nuclear and Particle Physics (INPP), NCSR Demokritos, Aghia Paraskevi, Greece
G. Anagnostou, G. Daskalakis, T. Geralis, V.A. Giakoumopoulou, A. Kyriakis, D. Loukas, I. Topsis-Giotis

National and Kapodistrian University of Athens, Athens, Greece
A. Agapitos, S. Kesisoglou, A. Panagiotou, N. Saoulidou, E. Tziaferi

University of Ioánnina, Ioánnina, Greece
I. Evangelou, G. Flouris, C. Foudas, P. Kokkas, N. Loukas, N. Manthos, I. Papadopoulos, E. Paradas

MTA-ELTE Lendület CMS Particle and Nuclear Physics Group, Eötvös Loránd University
N. Filipovic

Wigner Research Centre for Physics, Budapest, Hungary
G. Bencze, C. Hajdu, P. Hidas, D. Horvath[20], F. Sikler, V. Veszpremi, G. Vesztergombi[21], A.J. Zsigmond

Institute of Nuclear Research ATOMKI, Debrecen, Hungary
N. Beni, S. Czellar, J. Karancsi[22], J. Molnar, Z. Szillasi

University of Debrecen, Debrecen, Hungary
M. Bartók[21], A. Makovec, P. Raics, Z.L. Trocsanyi, B. Ujvari

National Institute of Science Education and Research, Bhubaneswar, India
S. Bahinipati, S. Choudhury[23], P. Mal, K. Mandal, A. Nayak, D.K. Sahoo, N. Sahoo, S.K. Swain

Panjab University, Chandigarh, India
S. Bansal, S.B. Beri, V. Bhatnagar, R. Chawla, R. Gupta, U.Bhawandeep, A.K. Kalsi, A. Kaur, M. Kaur, R. Kumar, A. Mehta, M. Mittal, J.B. Singh, G. Walia

University of Delhi, Delhi, India
Ashok Kumar, A. Bhardwaj, B.C. Choudhary, R.B. Garg, S. Keshri, A. Kumar, S. Malhotra, M. Naimuddin, N. Nishu, K. Ranjan, R. Sharma, V. Sharma

Saha Institute of Nuclear Physics, Kolkata, India
R. Bhattacharya, S. Bhattacharya, K. Chatterjee, S. Dey, S. Dutt, S. Dutta, S. Ghosh, N. Majumdar, A. Modak, K. Mondal, S. Mukhopadhyay, S. Nandan, A. Purohit, A. Roy, D. Roy, S. Roy Chowdhury, S. Sarkar, M. Sharan, S. Thakur

Indian Institute of Technology Madras, Madras, India
P.K. Behera

Bhabha Atomic Research Centre, Mumbai, India
R. Chudasama, D. Dutta, V. Jha, V. Kumar, A.K. Mohanty[15], P.K. Netrakanti, L.M. Pant, P. Shukla, A. Topkar

Tata Institute of Fundamental Research, Mumbai, India
T. Aziz, S. Banerjee, S. Bhowmik[24], R.M. Chatterjee, R.K. Dewanjee, S. Dugad, S. Ganguly, M. Guchait, A. Gurtu[25], Sa. Jain, G. Kole, S. Kumar, B. Mahakud, M. Maity[24], G. Majumder, K. Mazumdar, S. Mitra, G.B. Mohanty, B. Parida, T. Sarkar[24], N. Sur, B. Sutar, N. Wickramage[26]

Indian Institute of Science Education and Research (IISER), Pune, India
S. Chauhan, S. Dube, A. Kapoor, K. Kothekar, A. Rane, S. Sharma

Institute for Research in Fundamental Sciences (IPM), Tehran, Iran
H. Bakhshiansohi, H. Behnamian, S. Chenarani, E. Eskandari Tadavani, S.M. Etesami[27], A. Fahim[28], M. Khakzad, M. Mohammadi Najafabadi, M. Naseri, S. Paktinat Mehdiabadi, F. Rezaei Hosseinabadi, B. Safarzadeh[29], M. Zeinali

University College Dublin, Dublin, Ireland
M. Grunewald

INFN Sezione di Bari [a], Università di Bari [b], Politecnico di Bari [c], Bari, Italy
M. Abbrescia[a,b], C. Calabria[a,b], C. Caputo[a,b], A. Colaleo[a], D. Creanza[a,c], L. Cristella[a,b], N. De Filippis[a,c], M. De Palma[a,b], L. Fiore[a], G. Iaselli[a,c], G. Maggi[a,c], M. Maggi[a], G. Miniello[a,b], S. My[a,b], S. Nuzzo[a,b], A. Pompili[a,b], G. Pugliese[a,c], R. Radogna[a,b], A. Ranieri[a], G. Selvaggi[a,b], L. Silvestris[a,15], R. Venditti[a,b]

INFN Sezione di Bologna [a], Università di Bologna [b], Bologna, Italy
G. Abbiendi[a], C. Battilana, D. Bonacorsi[a,b], S. Braibant-Giacomelli[a,b], L. Brigliadori[a,b], R. Campanini[a,b], P. Capiluppi[a,b], A. Castro[a,b], F.R. Cavallo[a], S.S. Chhibra[a,b], G. Codispoti[a,b], M. Cuffiani[a,b], G.M. Dallavalle[a], F. Fabbri[a], A. Fanfani[a,b], D. Fasanella[a,b], P. Giacomelli[a], C. Grandi[a], L. Guiducci[a,b], S. Marcellini[a], G. Masetti[a], A. Montanari[a], F.L. Navarria[a,b], A. Perrotta[a], A.M. Rossi[a,b], T. Rovelli[a,b], G.P. Siroli[a,b], N. Tosi[a,b,15]

INFN Sezione di Catania [a], Università di Catania [b], Catania, Italy
S. Albergo[a,b], M. Chiorboli[a,b], S. Costa[a,b], A. Di Mattia[a], F. Giordano[a,b], R. Potenza[a,b], A. Tricomi[a,b], C. Tuve[a,b]

INFN Sezione di Firenze [a], Università di Firenze [b], Firenze, Italy
G. Barbagli[a], V. Ciulli[a,b], C. Civinini[a], R. D'Alessandro[a,b], E. Focardi[a,b], V. Gori[a,b], P. Lenzi[a,b], M. Meschini[a], S. Paoletti[a], G. Sguazzoni[a], L. Viliani[a,b,15]

INFN Laboratori Nazionali di Frascati, Frascati, Italy
L. Benussi, S. Bianco, F. Fabbri, D. Piccolo, F. Primavera[15]

INFN Sezione di Genova [a], Università di Genova [b], Genova, Italy
V. Calvelli[a,b], F. Ferro[a], M. Lo Vetere[a,b], M.R. Monge[a,b], E. Robutti[a], S. Tosi[a,b]

INFN Sezione di Milano-Bicocca [a], Università di Milano-Bicocca [b], Milano, Italy
L. Brianza, F. Brivio, M.E. Dinardo[a,b], S. Fiorendi[a,b], S. Gennai[a], A. Ghezzi[a,b], P. Govoni[a,b], S. Malvezzi[a], R.A. Manzoni[a,b,15], B. Marzocchi[a,b], D. Menasce[a], L. Moroni[a], M. Paganoni[a,b], D. Pedrini[a], S. Pigazzini, S. Ragazzi[a,b], T. Tabarelli de Fatis[a,b]

INFN Sezione di Napoli [a], Università di Napoli 'Federico II' [b], Napoli, Italy, Università della Basilicata [c], Potenza, Italy, Università G. Marconi [d], Roma, Italy
S. Buontempo[a], N. Cavallo[a,c], G. De Nardo, S. Di Guida[a,d,15], M. Esposito[a,b], F. Fabozzi[a,c], A.O.M. Iorio[a,b], G. Lanza[a], L. Lista[a], S. Meola[a,d,15], M. Merola[a], P. Paolucci[a,15], C. Sciacca[a,b], F. Thyssen

INFN Sezione di Padova [a], Università di Padova [b], Padova, Italy, Università di Trento [c], Trento, Italy
P. Azzi[a,15], N. Bacchetta[a], L. Benato[a,b], D. Bisello[a,b], A. Boletti[a,b], R. Carlin[a,b], A. Carvalho Antunes De Oliveira[a,b], P. Checchia[a], M. Dall'Osso[a,b], P. De Castro Manzano[a], T. Dorigo[a], U. Dosselli[a], F. Gasparini[a,b], U. Gasparini[a,b], A. Gozzelino[a], S. Lacaprara[a], M. Margoni[a,b], A.T. Meneguzzo[a,b], J. Pazzini[a,b,15], N. Pozzobon[a,b], P. Ronchese[a,b], F. Simonetto[a,b], E. Torassa[a], M. Tosi[a,b], M. Zanetti, P. Zotto[a,b], A. Zucchetta[a,b], G. Zumerle[a,b]

INFN Sezione di Pavia [a], Università di Pavia [b], Pavia, Italy
A. Braghieri[a], A. Magnani[a,b], P. Montagna[a,b], S.P. Ratti[a,b], V. Re[a], C. Riccardi[a,b], P. Salvini[a], I. Vai[a,b], P. Vitulo[a,b]

INFN Sezione di Perugia [a], Università di Perugia [b], Perugia, Italy
L. Alunni Solestizi[a,b], G.M. Bilei[a], D. Ciangottini[a,b], L. Fanò[a,b], P. Lariccia[a,b], R. Leonardi[a,b], G. Mantovani[a,b], M. Menichelli[a], A. Saha[a], A. Santocchia[a,b]

INFN Sezione di Pisa [a], Università di Pisa [b], Scuola Normale Superiore di Pisa [c], Pisa, Italy
K. Androsov[a,30], P. Azzurri[a,15], G. Bagliesi[a], J. Bernardini[a], T. Boccali[a], R. Castaldi[a], M.A. Ciocci[a,30], R. Dell'Orso[a], S. Donato[a,c], G. Fedi, A. Giassi[a], M.T. Grippo[a,30], F. Ligabue[a,c], T. Lomtadze[a], L. Martini[a,b], A. Messineo[a,b], F. Palla[a], A. Rizzi[a,b], A. Savoy-Navarro[a,31], P. Spagnolo[a], R. Tenchini[a], G. Tonelli[a,b], A. Venturi[a], P.G. Verdini[a]

INFN Sezione di Roma [a], Università di Roma [b], Roma, Italy
L. Barone[a,b], F. Cavallari[a], M. Cipriani[a,b], G. D'imperio[a,b,15], D. Del Re[a,b,15], M. Diemoz[a], S. Gelli[a,b], C. Jorda[a], E. Longo[a,b], F. Margaroli[a,b], P. Meridiani[a], G. Organtini[a,b], R. Paramatti[a], F. Preiato[a,b], S. Rahatlou[a,b], C. Rovelli[a], F. Santanastasio[a,b]

INFN Sezione di Torino [a], Università di Torino [b], Torino, Italy, Università del Piemonte Orientale [c], Novara, Italy
N. Amapane[a,b], R. Arcidiacono[a,c,15], S. Argiro[a,b], M. Arneodo[a,c], N. Bartosik[a], R. Bellan[a,b], C. Biino[a], N. Cartiglia[a], M. Costa[a,b], R. Covarelli[a,b], A. Degano[a,b], N. Demaria[a], L. Finco[a,b], B. Kiani[a,b], C. Mariotti[a], S. Maselli[a], E. Migliore[a,b], V. Monaco[a,b], E. Monteil[a,b], M.M. Obertino[a,b], L. Pacher[a,b], N. Pastrone[a], M. Pelliccioni[a], G.L. Pinna Angioni[a,b], F. Ravera[a,b], A. Romero[a,b], M. Ruspa[a,c], R. Sacchi[a,b], V. Sola[a], A. Solano[a,b], A. Staiano[a], P. Traczyk[a,b]

INFN Sezione di Trieste [a], Università di Trieste [b], Trieste, Italy
S. Belforte[a], V. Candelise[a,b], M. Casarsa[a], F. Cossutti[a], G. Della Ricca[a,b], C. La Licata[a,b], A. Schizzi[a,b], A. Zanetti[a]

Kyungpook National University, Daegu, Korea
D.H. Kim, G.N. Kim, M.S. Kim, S. Lee, S.W. Lee, Y.D. Oh, S. Sekmen, D.C. Son, Y.C. Yang

Chonbuk National University, Jeonju, Korea
H. Kim

Hanyang University, Seoul, Korea
J.A. Brochero Cifuentes, T.J. Kim

Korea University, Seoul, Korea
S. Cho, S. Choi, Y. Go, D. Gyun, S. Ha, B. Hong, Y. Jo, Y. Kim, B. Lee, K. Lee, K.S. Lee, S. Lee, J. Lim, S.K. Park, Y. Roh

Seoul National University, Seoul, Korea
J. Almond, J. Kim, S.H. Seo, U. Yang, H.D. Yoo, G.B. Yu

University of Seoul, Seoul, Korea
M. Choi, H. Kim, H. Kim, J.H. Kim, J.S.H. Lee, I.C. Park, G. Ryu, M.S. Ryu

Sungkyunkwan University, Suwon, Korea
Y. Choi, J. Goh, D. Kim, E. Kwon, J. Lee, I. Yu

Vilnius University, Vilnius, Lithuania
V. Dudenas, A. Juodagalvis, J. Vaitkus

National Centre for Particle Physics, Universiti Malaya, Kuala Lumpur, Malaysia
I. Ahmed, Z.A. Ibrahim, J.R. Komaragiri, M.A.B. Md Ali[32], F. Mohamad Idris[33], W.A.T. Wan Abdullah, M.N. Yusli, Z. Zolkapli

Centro de Investigacion y de Estudios Avanzados del IPN, Mexico City, Mexico
E. Casimiro Linares, H. Castilla-Valdez, E. De La Cruz-Burelo, I. Heredia-De La Cruz[34], A. Hernandez-Almada, R. Lopez-Fernandez, J. Mejia Guisao, A. Sanchez-Hernandez

Universidad Iberoamericana, Mexico City, Mexico
S. Carrillo Moreno, F. Vazquez Valencia

Benemerita Universidad Autonoma de Puebla, Puebla, Mexico
I. Pedraza, H.A. Salazar Ibarguen, C. Uribe Estrada

Universidad Autónoma de San Luis Potosí, San Luis Potosí, Mexico
A. Morelos Pineda

University of Auckland, Auckland, New Zealand
D. Krofcheck

University of Canterbury, Christchurch, New Zealand
P.H. Butler

National Centre for Physics, Quaid-I-Azam University, Islamabad, Pakistan
A. Ahmad, M. Ahmad, Q. Hassan, H.R. Hoorani, W.A. Khan, T. Khurshid, M. Shoaib, M. Waqas

National Centre for Nuclear Research, Swierk, Poland
H. Bialkowska, M. Bluj, B. Boimska, T. Frueboes, M. Górski, M. Kazana, K. Nawrocki, K. Romanowska-Rybinska, M. Szleper, P. Zalewski

Institute of Experimental Physics, Faculty of Physics, University of Warsaw, Warsaw, Poland
K. Bunkowski, A. Byszuk[35], K. Doroba, A. Kalinowski, M. Konecki, J. Krolikowski, M. Misiura, M. Olszewski, M. Walczak

Laboratório de Instrumentação e Física Experimental de Partículas, Lisboa, Portugal
P. Bargassa, C. Beirão Da Cruz E Silva, A. Di Francesco, P. Faccioli, P.G. Ferreira Parracho, M. Gallinaro, J. Hollar, N. Leonardo, L. Lloret Iglesias, M.V. Nemallapudi, F. Nguyen, J. Rodrigues Antunes, J. Seixas, O. Toldaiev, D. Vadruccio, J. Varela, P. Vischia

Joint Institute for Nuclear Research, Dubna, Russia
S. Afanasiev, P. Bunin, M. Gavrilenko, I. Golutvin, I. Gorbunov, A. Kamenev, V. Karjavin, A. Lanev, A. Malakhov, V. Matveev[36,37], P. Moisenz, V. Palichik, V. Perelygin, S. Shmatov, S. Shulha, N. Skatchkov, V. Smirnov, N. Voytishin, A. Zarubin

Petersburg Nuclear Physics Institute, Gatchina (St. Petersburg), Russia
L. Chtchipounov, V. Golovtsov, Y. Ivanov, V. Kim[38], E. Kuznetsova[39], V. Murzin, V. Oreshkin, V. Sulimov, A. Vorobyev

Institute for Nuclear Research, Moscow, Russia
Yu. Andreev, A. Dermenev, S. Gninenko, N. Golubev, A. Karneyeu, M. Kirsanov, N. Krasnikov, A. Pashenkov, D. Tlisov, A. Toropin

Institute for Theoretical and Experimental Physics, Moscow, Russia
V. Epshteyn, V. Gavrilov, N. Lychkovskaya, V. Popov, I. Pozdnyakov, G. Safronov, A. Spiridonov, M. Toms, E. Vlasov, A. Zhokin

National Research Nuclear University 'Moscow Engineering Physics Institute' (MEPhI), Moscow, Russia
M. Chadeeva, O. Markin, E. Tarkovskii

P.N. Lebedev Physical Institute, Moscow, Russia
V. Andreev, M. Azarkin[37], I. Dremin[37], M. Kirakosyan, A. Leonidov[37], S.V. Rusakov, A. Terkulov

Skobeltsyn Institute of Nuclear Physics, Lomonosov Moscow State University, Moscow, Russia
A. Baskakov, A. Belyaev, E. Boos, M. Dubinin[40], L. Dudko, A. Ershov, A. Gribushin, V. Klyukhin, O. Kodolova, I. Lokhtin, I. Miagkov, S. Obraztsov, S. Petrushanko, V. Savrin, A. Snigirev

State Research Center of Russian Federation, Institute for High Energy Physics, Protvino, Russia
I. Azhgirey, I. Bayshev, S. Bitioukov, D. Elumakhov, V. Kachanov, A. Kalinin, D. Konstantinov, V. Krychkine, V. Petrov, R. Ryutin, A. Sobol, S. Troshin, N. Tyurin, A. Uzunian, A. Volkov

University of Belgrade, Faculty of Physics and Vinca Institute of Nuclear Sciences, Belgrade, Serbia
P. Adzic[41], P. Cirkovic, D. Devetak, J. Milosevic, V. Rekovic

Centro de Investigaciones Energéticas Medioambientales y Tecnológicas (CIEMAT), Madrid, Spain
J. Alcaraz Maestre, E. Calvo, M. Cerrada, M. Chamizo Llatas, N. Colino, B. De La Cruz, A. Delgado Peris, A. Escalante Del Valle, C. Fernandez Bedoya, J.P. Fernández Ramos, J. Flix, M.C. Fouz, P. Garcia-Abia, O. Gonzalez Lopez, S. Goy Lopez, J.M. Hernandez, M.I. Josa, E. Navarro De Martino, A. Pérez-Calero Yzquierdo, J. Puerta Pelayo, A. Quintario Olmeda, I. Redondo, L. Romero, M.S. Soares

Universidad Autónoma de Madrid, Madrid, Spain
J.F. de Trocóniz, M. Missiroli, D. Moran

Universidad de Oviedo, Oviedo, Spain
J. Cuevas, J. Fernandez Menendez, I. Gonzalez Caballero, E. Palencia Cortezon, S. Sanchez Cruz, J.M. Vizan Garcia

Instituto de Física de Cantabria (IFCA), CSIC-Universidad de Cantabria, Santander, Spain
I.J. Cabrillo, A. Calderon, J.R. Castiñeiras De Saa, E. Curras, M. Fernandez, J. Garcia-Ferrero, G. Gomez, A. Lopez Virto, J. Marco, C. Martinez Rivero, F. Matorras, J. Piedra Gomez, T. Rodrigo, A. Ruiz-Jimeno, L. Scodellaro, N. Trevisani, I. Vila, R. Vilar Cortabitarte

CERN, European Organization for Nuclear Research, Geneva, Switzerland
D. Abbaneo, E. Auffray, G. Auzinger, M. Bachtis, P. Baillon, A.H. Ball, D. Barney, P. Bloch, A. Bocci, A. Bonato, C. Botta, T. Camporesi, R. Castello, M. Cepeda, G. Cerminara, M. D'Alfonso, D. d'Enterria, A. Dabrowski, V. Daponte, A. David, M. De Gruttola, F. De Guio, A. De Roeck, E. Di Marco[42], M. Dobson, M. Dordevic, B. Dorney, T. du Pree, D. Duggan, M. Dünser, N. Dupont, A. Elliott-Peisert, S. Fartoukh, G. Franzoni, J. Fulcher, W. Funk, D. Gigi, K. Gill, M. Girone, F. Glege, S. Gundacker, M. Guthoff, J. Hammer, P. Harris, J. Hegeman, V. Innocente, P. Janot, H. Kirschenmann, V. Knünz, M.J. Kortelainen, K. Kousouris, M. Krammer[1], P. Lecoq, C. Lourenço, M.T. Lucchini, N. Magini, L. Malgeri, M. Mannelli, A. Martelli, F. Meijers, S. Mersi, E. Meschi, F. Moortgat, S. Morovic, M. Mulders, H. Neugebauer, S. Orfanelli[43], L. Orsini, L. Pape, E. Perez, M. Peruzzi, A. Petrilli, G. Petrucciani, A. Pfeiffer, M. Pierini, A. Racz, T. Reis, G. Rolandi[44], M. Rovere, M. Ruan, H. Sakulin, J.B. Sauvan, C. Schäfer, C. Schwick, M. Seidel, A. Sharma, P. Silva, M. Simon, P. Sphicas[45], J. Steggemann, M. Stoye, Y. Takahashi, D. Treille, A. Triossi, A. Tsirou, V. Veckalns[46], G.I. Veres[21], N. Wardle, A. Zagozdzinska[35], W.D. Zeuner

Paul Scherrer Institut, Villigen, Switzerland
W. Bertl, K. Deiters, W. Erdmann, R. Horisberger, Q. Ingram, H.C. Kaestli, D. Kotlinski, U. Langenegger, T. Rohe

Institute for Particle Physics, ETH Zurich, Zurich, Switzerland
F. Bachmair, L. Bäni, L. Bianchini, B. Casal, G. Dissertori, M. Dittmar, M. Donegà, P. Eller, C. Grab, C. Heidegger, D. Hits, J. Hoss, G. Kasieczka, P. Lecomte†, W. Lustermann, B. Mangano, M. Marionneau, P. Martinez Ruiz del Arbol, M. Masciovecchio, M.T. Meinhard, D. Meister, F. Micheli, P. Musella, F. Nessi-Tedaldi, F. Pandolfi, J. Pata, F. Pauss, G. Perrin, L. Perrozzi, M. Quittnat, M. Rossini, M. Schönenberger, A. Starodumov[47], M. Takahashi, V.R. Tavolaro, K. Theofilatos, R. Wallny

Universität Zürich, Zurich, Switzerland
T.K. Aarrestad, C. Amsler[48], L. Caminada, M.F. Canelli, V. Chiochia, A. De Cosa, C. Galloni, A. Hinzmann, T. Hreus, B. Kilminster, C. Lange, J. Ngadiuba, D. Pinna, G. Rauco, P. Robmann, D. Salerno, Y. Yang

National Central University, Chung-Li, Taiwan
K.H. Chen, T.H. Doan, Sh. Jain, R. Khurana, M. Konyushikhin, C.M. Kuo, W. Lin, Y.J. Lu, A. Pozdnyakov, S.S. Yu

National Taiwan University (NTU), Taipei, Taiwan
Arun Kumar, P. Chang, Y.H. Chang, Y.W. Chang, Y. Chao, K.F. Chen, P.H. Chen, C. Dietz, F. Fiori, W.-S. Hou, Y. Hsiung, Y.F. Liu, R.-S. Lu, M. Miñano Moya, E. Paganis, J.f. Tsai, Y.M. Tzeng

Chulalongkorn University, Faculty of Science, Department of Physics, Bangkok, Thailand
B. Asavapibhop, G. Singh, N. Srimanobhas, N. Suwonjandee

Cukurova University, Adana, Turkey
A. Adiguzel, S. Cerci[49], S. Damarseckin, Z.S. Demiroglu, C. Dozen, I. Dumanoglu, S. Girgis, G. Gokbulut, Y. Guler, E. Gurpinar, I. Hos, E.E. Kangal[50], A. Kayis Topaksu, G. Onengut[51], K. Ozdemir[52], D. Sunar Cerci[49], B. Tali[49], C. Zorbilmez

Middle East Technical University, Physics Department, Ankara, Turkey
B. Bilin, S. Bilmis, B. Isildak[53], G. Karapinar[54], M. Yalvac, M. Zeyrek

Bogazici University, Istanbul, Turkey
E. Gülmez, M. Kaya[55], O. Kaya[56], E.A. Yetkin[57], T. Yetkin[58]

Istanbul Technical University, Istanbul, Turkey
A. Cakir, K. Cankocak, S. Sen[59], F.I. Vardarlı

Institute for Scintillation Materials of National Academy of Science of Ukraine, Kharkov, Ukraine
B. Grynyov

National Scientific Center, Kharkov Institute of Physics and Technology, Kharkov, Ukraine
L. Levchuk, P. Sorokin

University of Bristol, Bristol, United Kingdom
R. Aggleton, F. Ball, L. Beck, J.J. Brooke, D. Burns, E. Clement, D. Cussans, H. Flacher, J. Goldstein, M. Grimes, G.P. Heath, H.F. Heath, J. Jacob, L. Kreczko, C. Lucas, Z. Meng, D.M. Newbold[60], S. Paramesvaran, A. Poll, T. Sakuma, S. Seif El Nasr-storey, S. Senkin, D. Smith, V.J. Smith

Rutherford Appleton Laboratory, Didcot, United Kingdom
K.W. Bell, A. Belyaev[61], C. Brew, R.M. Brown, L. Calligaris, D. Cieri, D.J.A. Cockerill, J.A. Coughlan, K. Harder, S. Harper, E. Olaiya, D. Petyt, C.H. Shepherd-Themistocleous, A. Thea, I.R. Tomalin, T. Williams

Imperial College, London, United Kingdom
M. Baber, R. Bainbridge, O. Buchmuller, A. Bundock, D. Burton, S. Casasso, M. Citron, D. Colling, L. Corpe, P. Dauncey, G. Davies, A. De Wit, M. Della Negra, P. Dunne, A. Elwood, D. Futyan, Y. Haddad, G. Hall, G. Iles, R. Lane, C. Laner, R. Lucas[60], L. Lyons, A.-M. Magnan, S. Malik, L. Mastrolorenzo, J. Nash, A. Nikitenko[47], J. Pela, B. Penning, M. Pesaresi, D.M. Raymond, A. Richards, A. Rose, C. Seez, A. Tapper, K. Uchida, M. Vazquez Acosta[62], T. Virdee[15], S.C. Zenz

Brunel University, Uxbridge, United Kingdom
J.E. Cole, P.R. Hobson, A. Khan, P. Kyberd, D. Leslie, I.D. Reid, P. Symonds, L. Teodorescu, M. Turner

Baylor University, Waco, USA
A. Borzou, K. Call, J. Dittmann, K. Hatakeyama, H. Liu, N. Pastika

The University of Alabama, Tuscaloosa, USA
O. Charaf, S.I. Cooper, C. Henderson, P. Rumerio

Boston University, Boston, USA
D. Arcaro, A. Avetisyan, T. Bose, D. Gastler, D. Rankin, C. Richardson, J. Rohlf, L. Sulak, D. Zou

Brown University, Providence, USA
G. Benelli, E. Berry, D. Cutts, A. Ferapontov, A. Garabedian, J. Hakala, U. Heintz, O. Jesus, E. Laird, G. Landsberg, Z. Mao, M. Narain, S. Piperov, S. Sagir, E. Spencer, R. Syarif

University of California, Davis, Davis, USA
R. Breedon, G. Breto, D. Burns, M. Calderon De La Barca Sanchez, S. Chauhan, M. Chertok, J. Conway, R. Conway, P.T. Cox, R. Erbacher, C. Flores, G. Funk, M. Gardner, W. Ko, R. Lander, C. Mclean, M. Mulhearn, D. Pellett, J. Pilot, F. Ricci-Tam, S. Shalhout, J. Smith, M. Squires, D. Stolp, M. Tripathi, S. Wilbur, R. Yohay

University of California, Los Angeles, USA
R. Cousins, P. Everaerts, A. Florent, J. Hauser, M. Ignatenko, D. Saltzberg, E. Takasugi, V. Valuev, M. Weber

University of California, Riverside, Riverside, USA
K. Burt, R. Clare, J. Ellison, J.W. Gary, G. Hanson, J. Heilman, P. Jandir, E. Kennedy, F. Lacroix, O.R. Long, M. Malberti, M. Olmedo Negrete, M.I. Paneva, A. Shrinivas, H. Wei, S. Wimpenny, B. R. Yates

University of California, San Diego, La Jolla, USA
J.G. Branson, G.B. Cerati, S. Cittolin, R.T. D'Agnolo, M. Derdzinski, R. Gerosa, A. Holzner, R. Kelley, D. Klein, J. Letts, I. Macneill, D. Olivito, S. Padhi, M. Pieri, M. Sani, V. Sharma, S. Simon, M. Tadel, A. Vartak, S. Wasserbaech[63], C. Welke, J. Wood, F. Würthwein, A. Yagil, G. Zevi Della Porta

University of California, Santa Barbara, Santa Barbara, USA
R. Bhandari, J. Bradmiller-Feld, C. Campagnari, A. Dishaw, V. Dutta, K. Flowers, M. Franco Sevilla, P. Geffert, C. George, F. Golf, L. Gouskos, J. Gran, R. Heller, J. Incandela, N. Mccoll, S.D. Mullin, A. Ovcharova, J. Richman, D. Stuart, I. Suarez, C. West, J. Yoo

California Institute of Technology, Pasadena, USA
D. Anderson, A. Apresyan, J. Bendavid, A. Bornheim, J. Bunn, Y. Chen, J. Duarte, A. Mott, H.B. Newman, C. Pena, M. Spiropulu, J.R. Vlimant, S. Xie, R.Y. Zhu

Carnegie Mellon University, Pittsburgh, USA
M.B. Andrews, V. Azzolini, A. Calamba, B. Carlson, T. Ferguson, M. Paulini, J. Russ, M. Sun, H. Vogel, I. Vorobiev

University of Colorado Boulder, Boulder, USA
J.P. Cumalat, W.T. Ford, F. Jensen, A. Johnson, M. Krohn, T. Mulholland, K. Stenson, S.R. Wagner

Cornell University, Ithaca, USA
J. Alexander, A. Chatterjee, J. Chaves, J. Chu, S. Dittmer, N. Eggert, N. Mirman, G. Nicolas Kaufman, J.R. Patterson, A. Rinkevicius, A. Ryd, L. Skinnari, W. Sun, S.M. Tan, Z. Tao, W.D. Teo, J. Thom, J. Thompson, J. Tucker, Y. Weng, P. Wittich

Fairfield University, Fairfield, USA
D. Winn

Fermi National Accelerator Laboratory, Batavia, USA
S. Abdullin, M. Albrow, G. Apollinari, S. Banerjee, L.A.T. Bauerdick, A. Beretvas, J. Berryhill, P.C. Bhat, G. Bolla, K. Burkett, J.N. Butler, H.W.K. Cheung, F. Chlebana, S. Cihangir, M. Cremonesi, V.D. Elvira, I. Fisk, J. Freeman, E. Gottschalk, L. Gray, D. Green, S. Grünendahl, O. Gutsche, D. Hare, R.M. Harris, S. Hasegawa, J. Hirschauer, Z. Hu, B. Jayatilaka, S. Jindariani, M. Johnson, U. Joshi, B. Klima, B. Kreis, S. Lammel, J. Linacre, D. Lincoln, R. Lipton, T. Liu, R. Lopes De Sá, J. Lykken, K. Maeshima, J.M. Marraffino, S. Maruyama, D. Mason, P. McBride, P. Merkel, S. Mrenna, S. Nahn, C. Newman-Holmes†, V. O'Dell, K. Pedro, O. Prokofyev,

G. Rakness, L. Ristori, E. Sexton-Kennedy, A. Soha, W.J. Spalding, L. Spiegel, S. Stoynev, N. Strobbe, L. Taylor, S. Tkaczyk, N.V. Tran, L. Uplegger, E.W. Vaandering, C. Vernieri, M. Verzocchi, R. Vidal, M. Wang, H.A. Weber, A. Whitbeck

University of Florida, Gainesville, USA
D. Acosta, P. Avery, P. Bortignon, D. Bourilkov, A. Brinkerhoff, A. Carnes, M. Carver, D. Curry, S. Das, R.D. Field, I.K. Furic, J. Konigsberg, A. Korytov, P. Ma, K. Matchev, H. Mei, P. Milenovic[64], G. Mitselmakher, D. Rank, L. Shchutska, D. Sperka, L. Thomas, J. Wang, S. Wang, J. Yelton

Florida International University, Miami, USA
S. Linn, P. Markowitz, G. Martinez, J.L. Rodriguez

Florida State University, Tallahassee, USA
A. Ackert, J.R. Adams, T. Adams, A. Askew, S. Bein, B. Diamond, S. Hagopian, V. Hagopian, K.F. Johnson, A. Khatiwada, H. Prosper, A. Santra, M. Weinberg

Florida Institute of Technology, Melbourne, USA
M.M. Baarmand, V. Bhopatkar, S. Colafranceschi[65], M. Hohlmann, H. Kalakhety, D. Noonan, T. Roy, F. Yumiceva

University of Illinois at Chicago (UIC), Chicago, USA
M.R. Adams, L. Apanasevich, D. Berry, R.R. Betts, I. Bucinskaite, R. Cavanaugh, O. Evdokimov, L. Gauthier, C.E. Gerber, D.J. Hofman, P. Kurt, C. O'Brien, I.D. Sandoval Gonzalez, P. Turner, N. Varelas, Z. Wu, M. Zakaria, J. Zhang

The University of Iowa, Iowa City, USA
B. Bilki[66], W. Clarida, K. Dilsiz, S. Durgut, R.P. Gandrajula, M. Haytmyradov, V. Khristenko, J.-P. Merlo, H. Mermerkaya[67], A. Mestvirishvili, A. Moeller, J. Nachtman, H. Ogul, Y. Onel, F. Ozok[68], A. Penzo, C. Snyder, E. Tiras, J. Wetzel, K. Yi

Johns Hopkins University, Baltimore, USA
I. Anderson, B. Blumenfeld, A. Cocoros, N. Eminizer, D. Fehling, L. Feng, A.V. Gritsan, P. Maksimovic, M. Osherson, J. Roskes, U. Sarica, M. Swartz, M. Xiao, Y. Xin, C. You

The University of Kansas, Lawrence, USA
A. Al-bataineh, P. Baringer, A. Bean, C. Bruner, J. Castle, R.P. Kenny III, A. Kropivnitskaya, D. Majumder, M. Malek, W. Mcbrayer, M. Murray, S. Sanders, R. Stringer, Q. Wang

Kansas State University, Manhattan, USA
A. Ivanov, K. Kaadze, S. Khalil, M. Makouski, Y. Maravin, A. Mohammadi, L.K. Saini, N. Skhirtladze, S. Toda

Lawrence Livermore National Laboratory, Livermore, USA
D. Lange, F. Rebassoo, D. Wright

University of Maryland, College Park, USA
C. Anelli, A. Baden, O. Baron, A. Belloni, B. Calvert, S.C. Eno, C. Ferraioli, J.A. Gomez, N.J. Hadley, S. Jabeen, R.G. Kellogg, T. Kolberg, J. Kunkle, Y. Lu, A.C. Mignerey, Y.H. Shin, A. Skuja, M.B. Tonjes, S.C. Tonwar

Massachusetts Institute of Technology, Cambridge, USA
A. Apyan, R. Barbieri, A. Baty, R. Bi, K. Bierwagen, S. Brandt, W. Busza, I.A. Cali, Z. Demiragli, L. Di Matteo, G. Gomez Ceballos, M. Goncharov, D. Gulhan, D. Hsu, Y. Iiyama, G.M. Innocenti, M. Klute, D. Kovalskyi, K. Krajczar, Y.S. Lai, Y.-J. Lee, A. Levin, P.D. Luckey, A.C. Marini,

C. Mcginn, C. Mironov, S. Narayanan, X. Niu, C. Paus, C. Roland, G. Roland, J. Salfeld-Nebgen, G.S.F. Stephans, K. Sumorok, K. Tatar, M. Varma, D. Velicanu, J. Veverka, J. Wang, T.W. Wang, B. Wyslouch, M. Yang, V. Zhukova

University of Minnesota, Minneapolis, USA
A.C. Benvenuti, B. Dahmes, A. Evans, A. Finkel, A. Gude, P. Hansen, S. Kalafut, S.C. Kao, K. Klapoetke, Y. Kubota, Z. Lesko, J. Mans, S. Nourbakhsh, N. Ruckstuhl, R. Rusack, N. Tambe, J. Turkewitz

University of Mississippi, Oxford, USA
J.G. Acosta, S. Oliveros

University of Nebraska-Lincoln, Lincoln, USA
E. Avdeeva, R. Bartek, K. Bloom, S. Bose, D.R. Claes, A. Dominguez, C. Fangmeier, R. Gonzalez Suarez, R. Kamalieddin, D. Knowlton, I. Kravchenko, F. Meier, J. Monroy, J.E. Siado, G.R. Snow, B. Stieger

State University of New York at Buffalo, Buffalo, USA
M. Alyari, J. Dolen, J. George, A. Godshalk, C. Harrington, I. Iashvili, J. Kaisen, A. Kharchilava, A. Kumar, A. Parker, S. Rappoccio, B. Roozbahani

Northeastern University, Boston, USA
G. Alverson, E. Barberis, D. Baumgartel, M. Chasco, A. Hortiangtham, A. Massironi, D.M. Morse, D. Nash, T. Orimoto, R. Teixeira De Lima, D. Trocino, R.-J. Wang, D. Wood

Northwestern University, Evanston, USA
S. Bhattacharya, K.A. Hahn, A. Kubik, J.F. Low, N. Mucia, N. Odell, B. Pollack, M.H. Schmitt, K. Sung, M. Trovato, M. Velasco

University of Notre Dame, Notre Dame, USA
N. Dev, M. Hildreth, K. Hurtado Anampa, C. Jessop, D.J. Karmgard, N. Kellams, K. Lannon, N. Marinelli, F. Meng, C. Mueller, Y. Musienko[36], M. Planer, A. Reinsvold, R. Ruchti, N. Rupprecht, G. Smith, S. Taroni, N. Valls, M. Wayne, M. Wolf, A. Woodard

The Ohio State University, Columbus, USA
J. Alimena, L. Antonelli, J. Brinson, B. Bylsma, L.S. Durkin, S. Flowers, B. Francis, A. Hart, C. Hill, R. Hughes, W. Ji, B. Liu, W. Luo, D. Puigh, M. Rodenburg, B.L. Winer, H.W. Wulsin

Princeton University, Princeton, USA
O. Driga, P. Elmer, J. Hardenbrook, P. Hebda, D. Marlow, T. Medvedeva, M. Mooney, J. Olsen, C. Palmer, P. Piroué, D. Stickland, C. Tully, A. Zuranski

University of Puerto Rico, Mayaguez, USA
S. Malik

Purdue University, West Lafayette, USA
A. Barker, V.E. Barnes, D. Benedetti, S. Folgueras, L. Gutay, M.K. Jha, M. Jones, A.W. Jung, K. Jung, D.H. Miller, N. Neumeister, B.C. Radburn-Smith, X. Shi, J. Sun, A. Svyatkovskiy, F. Wang, W. Xie, L. Xu

Purdue University Calumet, Hammond, USA
N. Parashar, J. Stupak

Rice University, Houston, USA
A. Adair, B. Akgun, Z. Chen, K.M. Ecklund, F.J.M. Geurts, M. Guilbaud, W. Li, B. Michlin, M. Northup, B.P. Padley, R. Redjimi, J. Roberts, J. Rorie, Z. Tu, J. Zabel

University of Rochester, Rochester, USA
B. Betchart, A. Bodek, P. de Barbaro, R. Demina, Y.t. Duh, Y. Eshaq, T. Ferbel, M. Galanti, A. Garcia-Bellido, J. Han, O. Hindrichs, A. Khukhunaishvili, K.H. Lo, P. Tan, M. Verzetti

Rutgers, The State University of New Jersey, Piscataway, USA
J.P. Chou, E. Contreras-Campana, Y. Gershtein, T.A. Gómez Espinosa, E. Halkiadakis, M. Heindl, D. Hidas, E. Hughes, S. Kaplan, R. Kunnawalkam Elayavalli, S. Kyriacou, A. Lath, K. Nash, H. Saka, S. Salur, S. Schnetzer, D. Sheffield, S. Somalwar, R. Stone, S. Thomas, P. Thomassen, M. Walker

University of Tennessee, Knoxville, USA
M. Foerster, J. Heideman, G. Riley, K. Rose, S. Spanier, K. Thapa

Texas A&M University, College Station, USA
O. Bouhali[69], A. Castaneda Hernandez[69], A. Celik, M. Dalchenko, M. De Mattia, A. Delgado, S. Dildick, R. Eusebi, J. Gilmore, T. Huang, E. Juska, T. Kamon[70], V. Krutelyov, R. Mueller, Y. Pakhotin, R. Patel, A. Perloff, L. Perniè, D. Rathjens, A. Rose, A. Safonov, A. Tatarinov, K.A. Ulmer

Texas Tech University, Lubbock, USA
N. Akchurin, C. Cowden, J. Damgov, C. Dragoiu, P.R. Dudero, J. Faulkner, S. Kunori, K. Lamichhane, S.W. Lee, T. Libeiro, S. Undleeb, I. Volobouev, Z. Wang

Vanderbilt University, Nashville, USA
A.G. Delannoy, S. Greene, A. Gurrola, R. Janjam, W. Johns, C. Maguire, A. Melo, H. Ni, P. Sheldon, S. Tuo, J. Velkovska, Q. Xu

University of Virginia, Charlottesville, USA
M.W. Arenton, P. Barria, B. Cox, J. Goodell, R. Hirosky, A. Ledovskoy, H. Li, C. Neu, T. Sinthuprasith, X. Sun, Y. Wang, E. Wolfe, F. Xia

Wayne State University, Detroit, USA
C. Clarke, R. Harr, P.E. Karchin, C. Kottachchi Kankanamge Don, P. Lamichhane, J. Sturdy

University of Wisconsin - Madison, Madison, WI, USA
D.A. Belknap, S. Dasu, L. Dodd, S. Duric, B. Gomber, M. Grothe, M. Herndon, A. Hervé, P. Klabbers, A. Lanaro, A. Levine, K. Long, R. Loveless, I. Ojalvo, T. Perry, G.A. Pierro, G. Polese, T. Ruggles, A. Savin, A. Sharma, N. Smith, W.H. Smith, D. Taylor, P. Verwilligen, N. Woods

†: Deceased
1: Also at Vienna University of Technology, Vienna, Austria
2: Also at State Key Laboratory of Nuclear Physics and Technology, Peking University, Beijing, China
3: Also at Institut Pluridisciplinaire Hubert Curien, Université de Strasbourg, Université de Haute Alsace Mulhouse, CNRS/IN2P3, Strasbourg, France
4: Also at Universidade Estadual de Campinas, Campinas, Brazil
5: Also at Centre National de la Recherche Scientifique (CNRS) - IN2P3, Paris, France
6: Also at Université Libre de Bruxelles, Bruxelles, Belgium
7: Also at Deutsches Elektronen-Synchrotron, Hamburg, Germany
8: Also at Joint Institute for Nuclear Research, Dubna, Russia
9: Also at Helwan University, Cairo, Egypt
10: Now at Zewail City of Science and Technology, Zewail, Egypt
11: Also at Ain Shams University, Cairo, Egypt

12: Also at Fayoum University, El-Fayoum, Egypt
13: Now at British University in Egypt, Cairo, Egypt
14: Also at Université de Haute Alsace, Mulhouse, France
15: Also at CERN, European Organization for Nuclear Research, Geneva, Switzerland
16: Also at Skobeltsyn Institute of Nuclear Physics, Lomonosov Moscow State University, Moscow, Russia
17: Also at RWTH Aachen University, III. Physikalisches Institut A, Aachen, Germany
18: Also at University of Hamburg, Hamburg, Germany
19: Also at Brandenburg University of Technology, Cottbus, Germany
20: Also at Institute of Nuclear Research ATOMKI, Debrecen, Hungary
21: Also at MTA-ELTE Lendület CMS Particle and Nuclear Physics Group, Eötvös Loránd University, Budapest, Hungary
22: Also at University of Debrecen, Debrecen, Hungary
23: Also at Indian Institute of Science Education and Research, Bhopal, India
24: Also at University of Visva-Bharati, Santiniketan, India
25: Now at King Abdulaziz University, Jeddah, Saudi Arabia
26: Also at University of Ruhuna, Matara, Sri Lanka
27: Also at Isfahan University of Technology, Isfahan, Iran
28: Also at University of Tehran, Department of Engineering Science, Tehran, Iran
29: Also at Plasma Physics Research Center, Science and Research Branch, Islamic Azad University, Tehran, Iran
30: Also at Università degli Studi di Siena, Siena, Italy
31: Also at Purdue University, West Lafayette, USA
32: Also at International Islamic University of Malaysia, Kuala Lumpur, Malaysia
33: Also at Malaysian Nuclear Agency, MOSTI, Kajang, Malaysia
34: Also at Consejo Nacional de Ciencia y Tecnología, Mexico city, Mexico
35: Also at Warsaw University of Technology, Institute of Electronic Systems, Warsaw, Poland
36: Also at Institute for Nuclear Research, Moscow, Russia
37: Now at National Research Nuclear University 'Moscow Engineering Physics Institute' (MEPhI), Moscow, Russia
38: Also at St. Petersburg State Polytechnical University, St. Petersburg, Russia
39: Also at University of Florida, Gainesville, USA
40: Also at California Institute of Technology, Pasadena, USA
41: Also at Faculty of Physics, University of Belgrade, Belgrade, Serbia
42: Also at INFN Sezione di Roma; Università di Roma, Roma, Italy
43: Also at National Technical University of Athens, Athens, Greece
44: Also at Scuola Normale e Sezione dell'INFN, Pisa, Italy
45: Also at National and Kapodistrian University of Athens, Athens, Greece
46: Also at Riga Technical University, Riga, Latvia
47: Also at Institute for Theoretical and Experimental Physics, Moscow, Russia
48: Also at Albert Einstein Center for Fundamental Physics, Bern, Switzerland
49: Also at Adiyaman University, Adiyaman, Turkey
50: Also at Mersin University, Mersin, Turkey
51: Also at Cag University, Mersin, Turkey
52: Also at Piri Reis University, Istanbul, Turkey
53: Also at Ozyegin University, Istanbul, Turkey
54: Also at Izmir Institute of Technology, Izmir, Turkey
55: Also at Marmara University, Istanbul, Turkey
56: Also at Kafkas University, Kars, Turkey

57: Also at Istanbul Bilgi University, Istanbul, Turkey
58: Also at Yildiz Technical University, Istanbul, Turkey
59: Also at Hacettepe University, Ankara, Turkey
60: Also at Rutherford Appleton Laboratory, Didcot, United Kingdom
61: Also at School of Physics and Astronomy, University of Southampton, Southampton, United Kingdom
62: Also at Instituto de Astrofísica de Canarias, La Laguna, Spain
63: Also at Utah Valley University, Orem, USA
64: Also at University of Belgrade, Faculty of Physics and Vinca Institute of Nuclear Sciences, Belgrade, Serbia
65: Also at Facoltà Ingegneria, Università di Roma, Roma, Italy
66: Also at Argonne National Laboratory, Argonne, USA
67: Also at Erzincan University, Erzincan, Turkey
68: Also at Mimar Sinan University, Istanbul, Istanbul, Turkey
69: Also at Texas A&M University at Qatar, Doha, Qatar
70: Also at Kyungpook National University, Daegu, Korea